Catalysis Today 445 (2025) 115052

Contents lists available at ScienceDirect

Catalysis Today

journal homepage: www.elsevier.com/locate/cattod

Low-nuclearity single-atom and supported metal cluster catalysts in ethylene and propylene hydroformylation

Marcos G. Farpón, Gonzalo Prieto *

ITQ Instituto de Tecnología Química, Universitat Politècnica de València-Consejo Superior de Investigaciones Científicas (UPV-CSIC), Av. Los Naranjos s/n, Valencia 46022, Spain

ARTICLE INFO

Keywords:
Oxo-synthesis
Reactive separation
Single-atom catalysis
Metal cluster catalysis
Regioselectivity
Shape-selectivity

ABSTRACT

Olefin hydroformylation is one of the most significant examples of homogeneously catalyzed conversion processes. However, developing chemo/regio-selective and stable solid catalysts has remained a persistent challenge in heterogeneous catalysis. Particularly the design of solid catalysts for the hydroformylation of light, gaseous olefins, such as ethylene and propylene, has been extensively researched, given that the products from these processes are key players in the oxo-chemicals market. Additionally, developing selective, continuous gas-solid C_{2-3} olefin hydroformylation processes prospectively offers a reactive separation alternative to conventional and massively energy-intensive cryogenic distillation separation methods. In this review, we first assess the potential of reductive olefin hydroformylation as a cost-effective alternative to conventional cryogenic distillation processes for recovering value from industrial gas mixtures of ethylene and propylene. Taking a conventional ethylene splitter as a reference case, a reactive separation through ethylene reductive hydroformylation to 1-propanol is predicted to provide significant savings in terms of utility costs. Next, major advances in the design and development of solid catalysts for ethylene and propylene hydroformylation are surveyed, with an emphasis on single-atom catalysts (SACs) and supported metal nanoclusters. These catalysts have recently achieved hydroformylation activity and chemo/regio selectivity comparable to, or even surpassing, those traditionally exclusive to free molecular catalysts in solution. Different catalyst design strategies, including the heterogenization of metal coordination complexes in supported ionic liquid phase (SILP) catalysts and porous organic ligands (POLs), as well as the tuning of oxide-supported catalysts via the adjustment of metal-oxide interfacial effects or through nanoconfinement within zeolitic frameworks, are systematically reviewed and compared. Finally, conclusions are provided, alongside a critical perspective on fundamental and practical aspects that require particular attention to ensure rational and systematic progress toward optimized catalysts and reaction settings, ultimately paving the way for the heterogenization of light olefin hydroformylation processes.

1. Introduction

Hydroformylation (HF), also known as "oxo-synthesis," is a reaction of central industrial significance for converting C_n olefins into their C_{n+1} aldehyde derivatives by reaction with syngas ($CO+H_2$). Discovered by the German chemist Otto Roelen in the late 1930s, this reaction has since become foundational in the chemical industry. Roelen's work was built on earlier research with Franz Fischer on the Fischer-Tropsch synthesis (FTS) at the Kaiser Wilhelm Institute für Kohlenforschung (Mülheim an der Ruhr). They observed an increased formation of condensed oxygenated products when recycling olefins onto cobalt FTS catalysts. Later, Roelen refined this serendipitous discovery, and as research director at Ruhrchemie AG (Germany), he systematically transformed it into a landmark chemical process. Today, this technology is the largest example of industrialized homogeneous catalysis, employing molecular catalysts in solution [1]. Olefin hydroformylation is the dominant technology for the industrial production of aldehyde compounds, which are highly-demanded ingredients for chemical formulation in sectors spanning from the food, fragrances and flavors industry to pharma. Besides their end-use applications, aldehydes also play a key role as intermediates in the synthesis of other relevant chemicals such as alcohols, amines, carboxylic acids or esters, among other. It is estimated that the annual production for all these compounds, or *"oxo-chemicals"*, stands currently at around 10 Mt y^{-1} [2–6].

* Corresponding author.
E-mail address: prieto@itq.upv.es (G. Prieto).

https://doi.org/10.1016/j.cattod.2024.115052
Received 17 June 2024; Received in revised form 2 September 2024; Accepted 10 September 2024
Available online 11 September 2024
0920-5861/© 2024 The Author(s). Published by Elsevier B.V. This is an open access article under the CC BY-NC license (http://creativecommons.org/licenses/by-nc/4.0/).

Commercial hydroformylation processes are catalyzed either by Rh or Co-based (hydride)carbonyl coordination complexes in solution. A major challenge in HF processes is the design of catalysts offering high chemoselectivity to aldehyde products. An important side-reaction to inhibit is direct olefin hydrogenation, which is thermodynamically favored over hydroformylation and results in the formation of low-added value and chemically inert paraffin side-products. Therefore, achieving kinetic control is central to steer olefin conversion through hydroformylation pathways [7,8]. In specific cases, a second challenge is the control over regioselectivity. With the exception of ethylene and unfunctionalized cycloalkene substrates, hydroformylation products encompass a mixture of aldehyde isomer products, which correspond to Markovnikov and anti-Markovnikov additions of a formyl group to a C═C bond, as schematically illustrated in Fig. 1. Besides, increasingly complex mixtures of aldehyde products may be obtained when C═C bond isomerization reactions precede hydroformylation.

So far, the requisite activity and selectivity levels for commercial deployment have only been met using organometallic molecular complex catalysts in solution. The application of suitable organic ligands has long been the strategy to stabilize and tune the electronic and steric properties at the metal centers, affecting the energetics of transition states and thus providing means to adjust both activity and (regio) selectivity [3,5,9,10]. Several studies based on experiments and first-principle Density Functional Theory (DFT) calculations have proposed CO insertion into alkyl-metal bounds as the reaction's rate determining step (RDS) in the widely-accepted Heck-Breslow mechanism with neat Rh catalysts [11,12]. Various approaches, including ligand selection/engineering, the addition of co-catalysts and the modification of catalyst formulations with promoter compounds, have been successfully exercised to decrease the energy barrier for CO insertion. Thereby, higher reaction rates have been attained [13], and the need for high CO partial pressures for the development of HF-active metal (hydride)carbonyl species has been alleviated [14].

In its current technical implementation, olefin hydroformylation stands out as a prominent example of homogeneous catalysis. However, the development of solid-catalyzed HF processes represents an appealing endeavor, as it promises technically facile catalyst recovery and reuse. Minimizing net losses of catalyst in post-reaction sludges is generally a priority to prevent product contamination and maximize metal efficiency. This is especially critical in present times, which are marked by heightened price and marked cost volatility for metals like rhodium, which saw a staggering 40-fold increase in cost over the quinquennium from 2017 to 2021 [15,16]. Moreover, the realization of effective and stable solid catalysts opens the door to continuous vapor-solid processes in the gas-phase, particularly for volatile, light olefins.

Given their prospective potential to bridge the gap between traditional domains of homogeneous and heterogeneous catalysis by stabilizing active molecular motifs on solid matrices, single-atom catalysts (SACs), low-nuclearity sub-nm supported metal cluster catalysts, and materials based on supported liquid thin films have attracted significant attention in recent years as versatile platforms for developing (macroscopically) solid hydroformylation catalysts [17–19]. For reasons which shall be discussed in the following section, this review focuses on research efforts on the design of these families of materials as catalysts for the selective hydroformylation of light olefins, i.e. ethylene ($C_2^=$) and propylene ($C_3^=$), which currently represent around 70 % of the commercial oxo-synthesis processes.

Previous revisions have addressed hydroformylation catalysis using solid catalysts [7,12,21–24]. However, for gaseous C_{2-3} olefins, we consider that the process shows important particularities. Firstly, the irrelevance of olefin C═C isomerization side-reactions eliminates these concerns in catalyst development. Secondly, the process transcends its traditional conceptualization as an oxo-functionalization route. Therefore, it warrants specific attention in the present review article, which is organized as follows. Firstly, the potential of continuous, gas-solid heterogeneous catalysis in hydroformylation processes is highlighted as an alternative technology for recovering value from industrial gaseous mixtures containing ethylene/propylene (Section 2). Subsequently, a critical review of scientific literature is presented in Sections 3 and 4, focusing on the design and development of solid catalysts for ethylene and propylene hydroformylation based on supported low-nuclearity metal species. Finally, the authors provide their conclusions and perspectives on future research priorities in this area.

2. Gas-solid (reductive) olefin hydroformylation as a reactive separation method

Processes for converting ethylene and propylene into propanal and butanals, respectively, constitute the majority of today's industrial hydroformylation practice. Propylene hydroformylation is predominant in the sector due to the importance of butanals as intermediates in the synthesis of *n*-butanol and *2*-ethylhexanol, which are highly demanded precursors for solvents and plasticizers, respectively. In the case of ethylene hydroformylation, the installed capacity represents approximately 2 % of the global oxo-chemicals supply. Given the gaseous nature of the olefin reactants, adopting heterogeneous catalysis could enable continuous gas-solid conversions. However, achieving high chemo- and

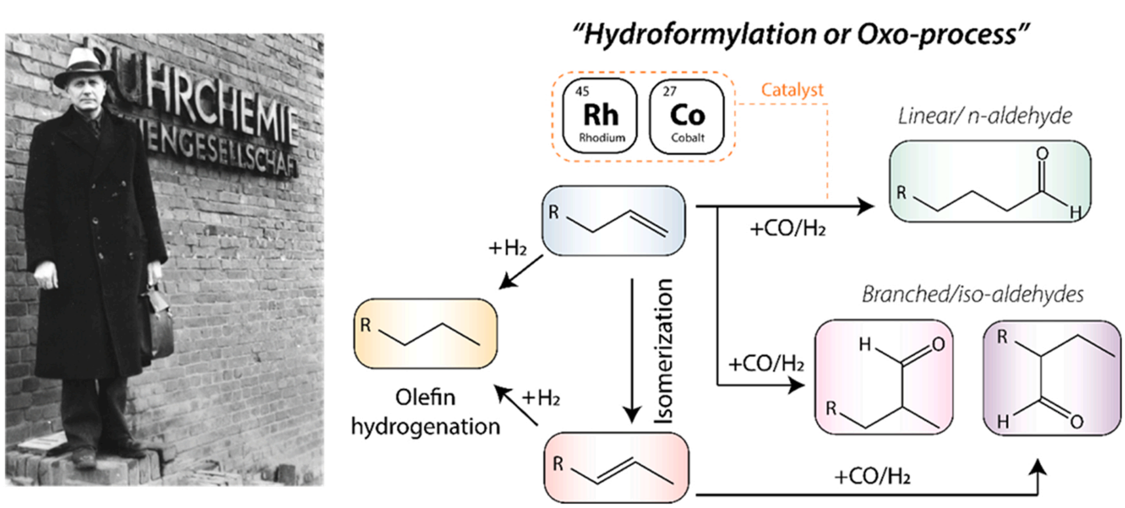

Fig. 1. General view of olefin hydroformylation or oxo-synthesis. Left, photograph of Otto Roelen in front of Ruhrchemie AG industries. Photograph extracted from © LVR Industriemuseum. Right, olefin conversion reactions, including hydroformylation and the undesired double-bond isomerization and hydrogenation pathways.

(in the case of propylene) regio-selectivity has proven challenging due to the increased reactivity of these short-chain olefins compared to longer-chain aliphatic olefins [12].

Currently, olefins are primarily generated through cracking processes like steam cracking (SC) and fluid catalytic cracking (FCC). However, the olefin yield from these processes tends to be relatively modest, typically falling below 70 % for ethylene and below 20 % for propylene production, depending on the specific hydrocarbon feedstock utilized [20,21]. Refinery off-gases are a relevant showcase, in which valorization is often economically unfeasible, leaving in many instances flaring, for heat production, as the sole alternative [22,23]. The recovery of light olefins from the outlet streams of crackers is challenging due to the complex mixture of hydrocarbon by-products in which they are diluted, necessitating additional separation units. One of the most challenging separations involves isolating olefins from their alkane counterparts, such as ethylene from ethane and propylene from propane. These separations are particularly difficult due to the similar molecular sizes (ranging from 4.16 to 4.50 Å) and boiling points (169 K and 184 K for the ethylene-ethane pair, and 225 K and 231 K for the propylene-propane pair, respectively). Attaining the stringent purity specifications required for further olefin use in various sectors, e.g. >99.5 % purity for polyolefin manufacture, adds to the complexity of these downstream separation processes [24,25].

Industrially, cryogenic distillation is the prevailing technology used to accomplish these separations. Ethylene-ethane and propylene-propane distillation columns, also known as C_2/C_3 "*splitters*" or "*fractionators*", are typically massive columns, comprising over 100 trays, each with an approximate cost of ca. 500 USD million. These columns are normally operated at pressures above atmospheric and cryogenic temperatures, approximately 2.3 MPa and 248 K for C_2, and 0.3 MPa and 243 K for C_3 splitters, respectively. Such operating conditions incur significant compression and cooling costs. In fact, the global energy demand linked to these separation processes was estimated to be ca. 10^{15} BTU y^{-1} (ca. 10^6 TJ y^{-1}) in the 90 s, roughly equivalent to the energy needs of a small country like Singapore [24–30].

In addition to their importance as an olefin oxo-functionalization route, continuous olefin (reductive) hydroformylation processes are of interest as a prospective *reactive separation* method for recovering chemical value from industrial gas streams where ethylene and/or propylene are diluted with low-value alkanes. This interest is primarily due to the significantly lower vapor pressure of the C_{n+1} oxygenated products compared to the initial olefinic substrates and their alkane counterparts. As depicted in Fig. 2.a under normal pressure conditions, the boiling point differences are relatively minor for C_2 and C_3 alkane/alkene pairs. However, for the corresponding C_3 and C_4 aldehyde olefin derivatives, the boiling points are significantly higher—specifically, 139 K and 117 K higher, respectively—compared to their corresponding paraffins. This boiling point difference is further increased if aldehydes are hydrogenated to the corresponding alcohol products, either in a separate selective hydrogenation stage, or via the coupling of hydroformylation and carbonyl selective hydrogenation in a single-step "*reductive hydroformylation*" (RedHF) process [31,32]. These marked differences in volatility could significantly facilitate the separation of the oxygenated olefin derivatives from the corresponding low-value alkane compounds, which would remain unreactive under (Red)HF conditions.

To illustrate the potential benefits of this alternative reactive separation, a simplified process simulation and techno-economic evaluation were performed, with the results presented in Fig. 2 and Table 1. An ethylene-ethane splitter was chosen as the base case, as this is one of the most energy-intensive separations in a conventional cryogenic distillation plant and a major contributor to the overall utility costs. The feed stream considered is an ethylene/ethane gas mixture with a molar composition of 85:15 ethylene to ethane, at a flow rate of 2385 kmol h^{-1} (equivalent to 500 kt of ethylene per year) [33]. Two case studies have been simulated: (i) a conventional ethylene-ethane splitter column, operating at representative conditions (feed conditions: P=2.1 MPa, T=249 K); and (ii) a gas-solid catalytic reductive hydroformylation process, operated in a fixed-bed reactor (P=2.1 MPa, T=383 K), at full ethylene conversion to *n*-propanol per reactor pass, followed by alcohol recovery.

For the case of a conventional *splitter*, utility costs have been estimated based on the heating and cooling duties at the reboiler and condenser, respectively. Propylene, sourced from the cascade refrigeration cycle at temperatures of 271 K and 238 K, is employed as the heat transfer fluid [33–36]. In the case of the RedHF process, the

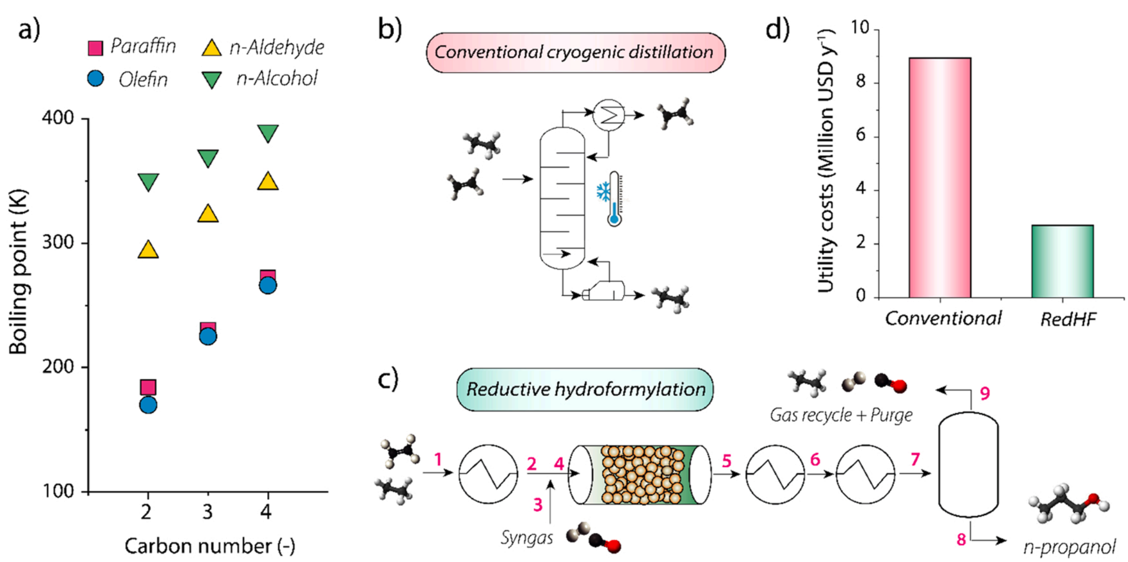

Fig. 2. a) Boiling point (at atmospheric pressure) for $C_{2\text{-}4}$ paraffin, olefin, *n*-aldehyde and *n*-alcohol compounds as a function of the carbon chain-length. b,c) Schematic process design and d) comparison of utility costs estimated for the separation of ethylene from a mixture with ethane using b) conventional cryogenic distillation and **c)** ethylene reductive hydroformylation (RedHF) to *n*-propanol as a reactive separation process, followed by *n*-propanol recovery in a flash separation step. On panel **c**, the temperature of those streams marked on the process scheme is as follows: T_1= 249 K, T_2=T_3=T_4=T_5=383 K, T_6=313 K, T_7=T_8=T_9=303 K. Further details on the simulations performed are provided in Table 1. Additional details on the process flow diagrams and streams are provided in Fig. S1 in the Supporting Information.

Table 1
Power consumption and utility costs estimation, per process unit, in a process of e conventional cryogenic distillation of a gas mixture of ethylene and ethane (C_2H_4:C_2H_6=85:15, molar), and a reactive recovery of the added-value compound from said mixture based on the reductive hydroformylation (RedHF) of ethylene to *n*-propanol. The estimation of the power consumption was obtained via simulation with Aspen-Hysys v.12.1, using the Peng-Robinson-Stryjek-Vera (PRSV) equation of state. For the cryogenic distillation process option, a tower of 140 ideal trays was simulated with the feed entering in tray 100 at T=249 K and P=2.1 MPa, assuming a total condenser. The condenser and reboiler are assumed to operate at T=243 K, P=1.93 MPa and T=265 K, P=1.95 MPa, respectively. The column was solved for an ethylene recovery and purity in the distillate of 99.9 %. In the case of the RedHF reactive recovery process, heater and cooler modules were considered for the estimation of the power consumption of the preheater and chillers after the reactor. The coolant demand for the RedHF reactor was estimated using a conversion reactor operating at 100 % ethylene conversion, with full selectivity to *n*-propanol, per pass. For the flash drum recovery of 2-propanol from inert ethane, a 2-phase separator has been considered.

Conventional cryogenic distillation process	Q (kW)	Thermal fluid	Mass/Volumetric Flowrate	Individual cost[d]	Annual cost (million USD)
Condenser	$1.98•10^4$	Propylene, 238 K	n.a.[a]	10.6 USD GJ^{-1}	6.6
Reboiler	$1.34•10^4$	Propylene, 271 K	n.a.	5.4 USD GJ^{-1}	2.3
				TOTAL	8.9
Reactive RedHF recovery process					
Preheater	$4.80•10^3$	LP Steam (0.103 MPag, 393 K)	2.2 kg s^{-1}[b]	29.3 USD t^{-1}	$2.01•10^{-3}$
Reactor coolant	$1.14•10^5$	Cooling water, 303 K	$2.71•10^3$ kg s^{-1}[c]	0.0148 USD m^{-3}	1.3
Chiller 1	$4.24•10^4$	Cooling water, 303 K	$1.01•10^3$ kg s^{-1}[c]	0.0148 USD m^{-3}	0.5
Chiller 2	$3.54•10^3$	Chilled water, 278 K	n.a.	4.4 USD GJ^{-1}	0.5
				TOTAL	2.2

[a] n.a.: " *Not applicable*", as for the cost estimation only the heating/cooling duty and cost per GJ was employed.
[b] Estimated from the preheater duty and the latent heat of vaporization for saturated steam at P=0.2 MPa and T=393 K (i.e. 2201 kJ kg^{-1}).
[c] Estimated from the corresponding chiller duty, the specific heat of water at constant pressure (i.e. 4.18 kJ kg^{-1} K^{-1} assuming constant value within the relevant temperature range) and the temperature gradient of the coolant across the heat exchanger, assumed to be 10 K as a well-accepted value in literature [105].
[d] Individual costs, as previously reported in [106,107].

ethylene-ethane stream is initially preheated to a reaction temperature of 383 K, in a heat exchanger using low-pressure steam. The reaction temperature of 383 K was selected for the reductive hydroformylation as it has been identified as optimal for highly selective solid Rh/SnO_2 single-atom-ethylene hydroformylation catalysts [37]. This stream is then combined with syngas (H_2:CO=2) in appropriate proportions to achieve a CO:ethylene molar ratio of 5. The resulting mixture serves as the feed stream to the RedHF reactor, which is assumed to operate at full ethylene conversion. The effluent from the reactor, comprising *n*-propanol, ethane, and unreacted syngas, is cooled down to 313 K in a first heat exchanger using cooling water at 303 K, and further down to 303 K in a second heat exchanger fed with chilled water at 278 K. Under the resulting stream conditions (P= 2.1 MPa, T= 303 K), over 97 % of the produced *n*-propanol can be readily recovered in a flash drum, attaining an alcohol purity >99.4 %.

As summarized in Fig. 2.d and Table 1, utility costs predicted for the alternative RedHF process are approximately four times lower than those incurred in the conventional cryogenic distillation. Additionally, the former potentially offers savings in terms of capital costs, as the recovery of *n*-propanol from the reaction mixture would not require a distillation column, in contrast to the massive tower which is characteristic of conventional ethylene-ethane *splitters*. While additional process integration aspects have not been considered, this simplified *in silico* comparison sufficiently underscores the potential advantages of gas-solid continuous RedHF processes as a reactive separation for the valorization of olefin-containing streams.

3. Solid catalysts for ethylene hydroformylation

Ethylene hydroformylation produces propanal as a single product. Under specific reaction conditions and depending on the nature of the catalyst, propanal may react further, *in situ*, to *n*-propanol or 2-methyl-2-pentenal (and derivatives thereof) via secondary aldehyde hydrogenation and self-aldol condensation reactions, respectively. Low-value ethane can also form via the thermodynamically favored olefin hydrogenation pathway. In the absence of additional considerations, such as regioselectivity, which is not of concern in ethylene hydroformylation, attaining sufficient chemoselectivity via the inhibition of olefin hydrogenation has long remained a central goal, but also a substantial challenge, for the development of solid ethylene hydroformylation catalysts.

3.1. Rh-based ethylene hydroformylation catalysts

Commercial processes for light (C_{4-}) olefin hydroformylation primarily use Rhodium (Rh) molecular catalysts due to their superior activity and selectivity at milder temperatures and lower pressures compared to alternative Co-based catalysts. Consequently, rhodium has also emerged as the preferred active metal in research efforts aimed at developing solid catalyst alternatives.

The Supported Ionic Liquid Phase (SILP) concept provides a strategy to heterogenize molecular catalysts without renouncing their most active free-standing state, in a liquid environment [38]. This class of materials is macroscopically solid, and thereby associated to technical benefits in terms of catalyst handling and amenability for continuous processes, while the free molecular catalyst is solubilized within a thin liquid film (ca. 1 nm) of an ionic liquid [39], i.e. with essentially null vapor pressure, coated on a solid carrier. Olefin hydroformylation has been a central process to showcase the SILP concept in continuous gas-solid conversion processes [38,40,41]. Weiß et al. synthesized a SILP catalyst bearing a Rh-Xantphos coordination complex dissolved in a thin film of 1-ethyl-3-methylimidazolium bis(trifluoromethylsulfonyl) imide ([EMIM][NTf_2]) coated on a nitrogen-doped carbon carrier [42]. The performance of this catalyst was evaluated in a packed-bed reactor for ethylene HF. Good hydroformylation activity (TOF=100 h^{-1}) was registered at 393 K, remarkably alongside full selectivity to hydroformylation. Ha et al. reported an alternative system consisting in a silica-supported Rh complex coordinated with TPPTS-Cs_3 (triphenylphosphine trisulfonate cesium) and dissolved in the [BMIm][n-$C_8H_{17}OSO_3$] (1-butyl-3-methylimidazolium octylsulfate) ionic liquid [43]. This catalyst attained a substantially higher TOF of 800 h^{-1} and selectivity of 90 % at 363 K, marking, to the authors' knowledge, the best performance reported for the SILP-catalyzed ethylene hydroformylation. While conceptually very elegant and fundamentally successful, the SILP technology has also been shown to face some challenges for a large-scale implementation, including the technically-complex handling of the supported liquid, sluggish reactant and product mass transfer across the ionic liquid film, as well as catalyst deactivation driven by the accumulation of heavy oxygenate side-products which, due to a limited vapor pressure, do not evaporate easily from the supported liquid film [7].

The desire to circumvent those limitations inherent to supported liquid films, while retaining the stabilization and promotional roles of organic ligands in molecular Rh catalysts, has turned the attention to soft-matter porous solids as hosts for supported Rh catalysts. The resulting solid catalysts are intended to integrate a full solid character with the mimicry of effective ligand-Rh coordination at the molecular level. The use of Porous Organic Polymers (POPs) is one of the strategies that has been explored for the stabilization of isolated Rh sites as olefin hydroformylation catalysts. Jiang et al. reported a Rh single-site catalyst supported on a *Porous Organic Ligand* (POL) synthesized via solvothermal polymerization of vinyl-functionalized triphenylphosphine (PPh_3) ligands [44]. Catalytic results for the gas-phase hydroformylation of ethylene revealed remarkably high activity (TOF>10^4 h^{-1}) and selectivity ($S_{PROPANAL}$=95.4 %) at 393 K, comparable to those performance figures characteristic of optimized molecular Rh catalysts in solution. On the basis of this remarkable performance, a demonstration site has been reportedly constructed and operated by Ningbo Juhua Chemical Technology Co., LTD (People's Republic of China), with a yearly capacity of 50 kt ethylene. In this process, ethylene is first converted to propanal by hydroformylation on the newly developed Rh-POL solid catalyst, followed by subsequent hydrogenation to *n*-propanol in a downstream, Ni-catalyzed hydrogenation step [45,46].

While SILP and soft-matter solid catalysts have provided good perspectives to effectively heterogenize olefin hydroformylation processes, inorganic solid catalysts are generally preferred for industrial deployment, owing to their cost-effective and established manufacture procedures, and greater thermal, chemical and mechanical stabilities. However, most oxide-supported Rh catalysts reported for ethylene hydroformylation have only partially addressed the challenge of attaining technically relevant chemoselectivity. This is exemplified in Fig. 5, which shows a survey of performance indicators reported for several ethylene hydroformylation catalytic systems. Particularly for those inorganic solid catalysts which have shown greater activities, e.g. metal-specific reaction rates >20 h^{-1}, the selectivity to propanal has remained <70 %, limited by the higher activity of these catalysts for ethylene hydrogenation compared to their molecular counterparts.

The consideration that olefins can form pi-bonded adspecies on extended metallic surfaces, coupled with the presumed central role of this adsorption mode in olefin hydrogenation catalysis [47], has shifted the focus to low-nuclearity metal active centers, such as isolated metal atoms and few-atom clusters. Unlike metal nanoparticles, these centers do not provide metal facets for olefin activation. Catalyzed by the emergence of higher precision catalyst synthesis methods as well as a wider access to X-ray absorption spectroscopy (XAS) and aberration-corrected (scanning) transmission electron microscopy (AC-(S)TEM) structural diagnostic methods, the last two decades have witnessed significant advances in the stabilization and engineering of low-nuclearity Rh species onto solid carrier materials. The extensive interfacial interaction of these ultrasmall metal motifs with the support confers the latter a role which extends beyond that of a carrier, and it conceptually approaches that of a *solid ligand*, by analogy with organometallic catalysts [48–51].

Amsler et al. studied oxide-supported Rh SACs as olefin hydroformylation catalysts, with complementary computational and experimental approaches [52]. The active site was modelled as a Rh hydride-dicarbonyl complex adsorbed on selected oxide surfaces. Using high-level DLPNO–CCSD(T) calculations, high ethylene hydroformylation rates were predicted for a Rh_1/CeO_2 catalyst. In contrast, Rh_1/MgO was predicted to display lower reactivity, in view of the higher energy barriers computed for CO insertion into the Rh-alkyl bond. Experimentally, XAS and AC-STEM results suggested that the lower activity of Rh_1/MgO, which was experimentally verified in the hydroformylation of styrene, could be ascribed to a higher degree of confinement of the mononuclear Rh sites by the MgO support, i.e. a higher average Rh-O coordination number. Collectively, the theoretical and experimental results suggested the potential of oxide-supported Rh SACs for olefin hydroformylation. Additionally, they underscored the importance of striking a trade-off between the stabilization of the Rh_1 centers by coordination to lattice oxygen "ligands" and a certain conformational flexibility at the metal atom to achieve olefin hydroformylation activity.

In a series of studies, Christopher and co-workers reported on Rh_1-MO_x interfacial sites supported on γ-Al_2O_3. In a first study, Rh_1-ReO_x sites were studied [53]. Interaction with the rhenium oxide clusters was found to modify the electronic properties of the Rh centers, leading to enhanced hydroformylation performance as evidenced by a correlation between the CO stretching frequencies in the $Rh(CO)_2$ species and HF activity. Periodic DFT calculations (PBE-D3) conducted on Rh_1 and Rh_1-Re_1O_x model sites on γ-Al_2O_3(110) [54], indicated that the neighboring ReO_x Lewis acid site weakened rhodium's π-donor ability and consequently diminished Rh-CO binding. This attenuation of the Rh-CO binding was anticipated to significantly impact the rate-limiting step in the HF mechanism, transitioning from CO insertion into the ethyl-Rh bond for the Re-free comparative site to the coordination of a second CO molecule to Rh for the Rh_1-ReO_x bimetallic site. In a subsequent investigation, Rh_1-WO_x pair sites were examined [55]. The findings revealed that, unlike Rh_1-ReO_x sites, surface tungstate species in proximity to atomically dispersed Rh experienced partial reduction upon exposure to ethylene and CO reactants. This observation suggested the potential for a bifunctional mechanism, involving both tungsten reduction and ethylene hydroformylation cycles. In this mechanistic proposal, the Rh-WO_x pair sites facilitated the transfer of ethylene from tungsten to rhodium without the need to desorb a CO molecule (Fig. 3). In addition, H_2 dissociation was predicted to occur at the interface between the Rh atom and the partially reduced tungstate species, lowering the hydrogen coverage on Rh and enabling the coordination of a third CO molecule which lowers the energetics for CO insertion. These mechanistic effects were in line with the high activity (TOF=32 h^{-1}) and propanal selectivity values (93 %) observed experimentally.

Independently, Farpón et al. studied metal oxide support effects in Rh SACs and exploited them to attain a selective ethylene hydroformylation in the gas-phase [56]. Out of a set of atomically dispersed Rh_1/MO_2 catalysts, the study illuminated the unconventional performance of Rh_1/SnO_2. This catalyst exhibited excellent ethylene hydroformylation activity (TOF=100–225 h^{-1}) while simultaneously offering nearly full selectivity to hydroformylation (95–99 %), through an effective inhibition of ethylene hydrogenation. By combining catalysis experiments with *in situ* spectroscopic investigations (CO-FTIR, XAS, Raman) and periodic DFT calculations (PBE-D3), the unique performance of Rh_1/SnO_2 was ascribed to its capacity to form oxygen vacancies in the direct vicinity of the Rh sites at remarkably mild reaction temperatures (ca. 383 K). Partial *de-ligation* of the Rh center upon departure of lattice oxygen, alongside interfacial H_2 dissociation, were predicted to facilitate the development of a Rh-monohydride complex (structure 1 in Fig. 4), which was experimentally detected with CO-FTIR. This resting active site was proposed to show a coordination pliability at the Rh atom resemblant of that in organometallic complexes. This feature enables its involvement in a classical Heck-Breslow reaction mechanism, characterized by low free energy barriers (47 kJ mol^{-1}) for oxidative ethylene addition into Rh-H and for CO insertion into Rh-ethyl species (57 kJ mol^{-1}) and a comparatively higher barrier for hydrogen insertion (105 kJ mol^{-1}), which account for the exceptionally high activity and selectivity observed in the gas-phase hydroformylation of ethylene.

Alternatively to regular oxides, zeotype molecular sieves, notably zeolites, have also received a significant attention as hosts for the stabilization of low-nuclearity metal species such as isolated metal atoms and clusters [57–59]. The use of zeolites as a host provides an exceedingly regular architecture, and a well-defined nano environment which may be exploited to induce stability to the confined metal species, and steric effects by the establishment of dispersion force interactions between reactants and reaction intermediates and the pore walls of the inorganic host. Qi et al. investigated the use of Rh sites grafted on ≡SiOM−OH (M=Zn or Co) nests generated in a dealuminated BEA

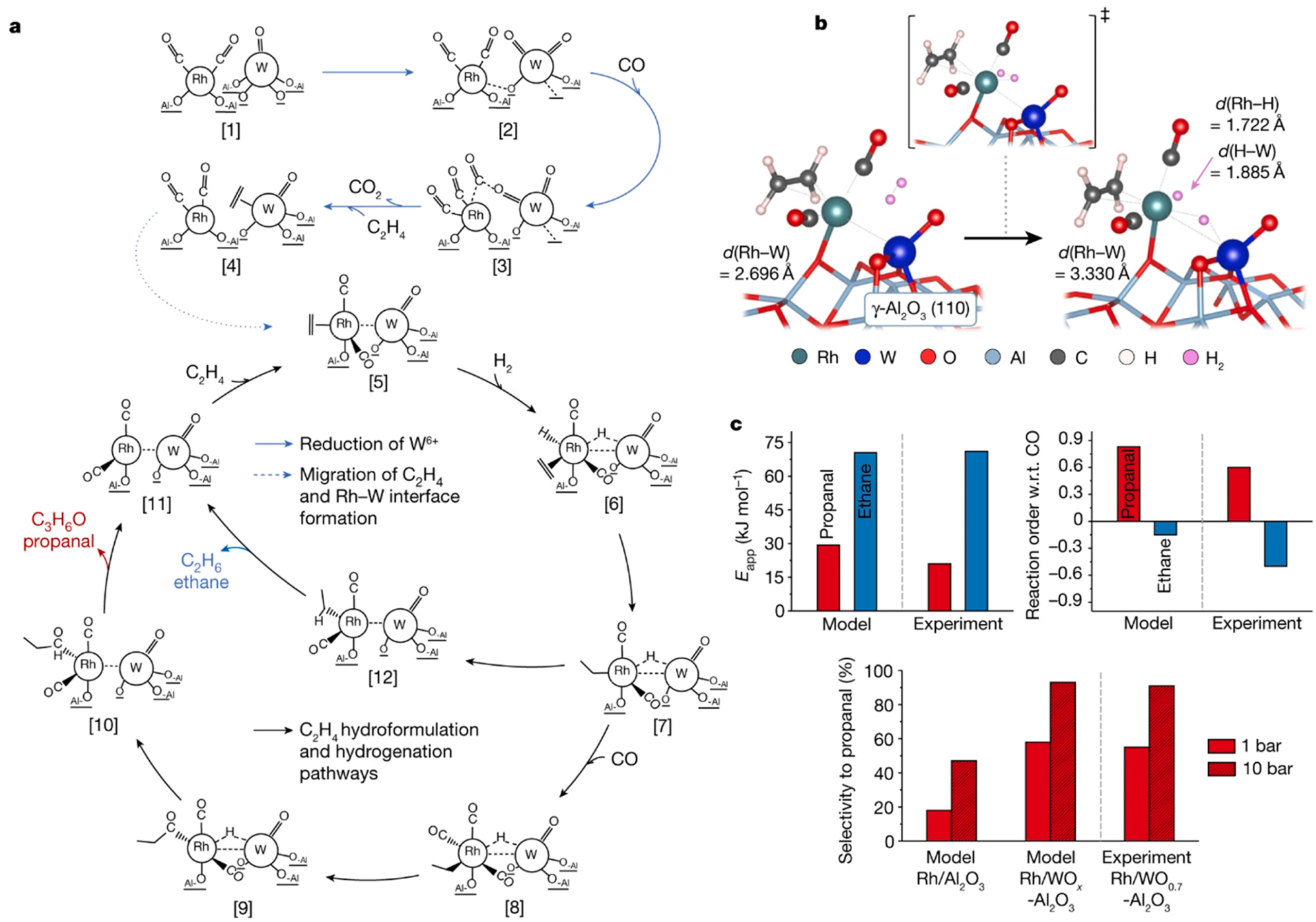

Fig. 3. a) Proposed mechanism of W^{6+} reduction by CO and catalytic cycles for ethylene hydroformylation and hydrogenation on a Rh-WO_x pair site supported on γ-Al_2O_3. In contrast to Rh/Al_2O_3, activation of the catalyst does not require desorption of a CO ligand, and H_2 activation occurs at the Rh–W interface. b) The activated state of the catalyst after ethylene migration from W to Rh, formation of Rh–W bond (Rh–W ≈ 2.7 Å) and H_2 coordination at the Rh–W interface (left); the cooperative binuclear H_2 dissociation transition state (middle); dissociated 2 H* on Rh atom and Rh–W interface (right). **c**) Comparison of kinetic parameters from experiment and microkinetic simulations: apparent activation energy, E_{app} (top left); reaction order with respect to (w.r.t.) CO for product formation (top right); selectivity to propanal at 1 and 1.0 MPa total pressure on Rh/Al_2O_3 and Rh-WO_x/Al_2O_3 at 403 K (bottom).
Reproduced from [55], copyright (2022), with permission from Springer Nature.

zeolite [60]. The fraction of atomically dispersed Rh species scaled up with increasing amounts of the second metal M, indicative for the role of the latter to stabilize isolated Rh atoms. The ethylene hydroformylation rate per unit total Rh atom also increased. When M=Co, TOF values up to 153 h^{-1} were achieved, albeit with a moderate selectivity to propanal (69 %). In contrast, selecting Zn as the second metal increased selectivity propanal selectivity to 79 %, at expense of a decreased activity (TOF=12 h^{-1}). Zhao et al. [61] reported a (phosphorus-modified-) Rh/MFI catalyst. To overcome the inherent instability of Rh sites, the authors suggested a one-pot synthesis. In this method, a Rh-ethylenediamine complex and tetraethylphosphonium hydroxide, acting as a phosphorus-sourcing organic structure-directing agent (SDA), are simultaneously introduced into the aqueous media used for the crystallization of the MFI zeolite support. Following air-calcination of the organic SDA and catalyst thermal activation under either hydrogen or syngas flow, the samples were exposed to ethylene HF conditions. This resulted in the formation of phosphate species confined to the zeolite micropores, which stabilized the metal centers via Rh-O═P or Rh-O(H)-P interactions. The Rh/P-MFI catalyst achieved an Rh-specific ethylene hydroformylation rate of ca. 70 h^{-1}, in combination with a selectivity to propanal of 95 %. The authors attributed the catalytic performance to the phosphorus-assisted stabilization of high-oxidation (Rh^{3+}) species, acting as active sites for hydroformylation. This challenges the prevailing notion that oxidative additions onto the Rh center, often assumed to be formally Rh^{1+} in its resting state (e.g., a Rh (hydride)dicarbonyl), are essential early reaction steps for olefin hydroformylation.

Fig. 5 summarizes the current state of Rh-catalyzed ethylene hydroformylation. Additional details can be found in Table S2 in the Supporting Information. While the primary focus of this data survey is on catalysts comprising supported sub-nanometric Rh species, catalysts containing metal aggregates, such as nanoparticles, have also been considered for comparison. Additionally, relevant examples of molecular catalysts, including those dissolved in SILP thin-film layers or stabilized within POP soft matter frameworks, have been included as a benchmark. As illustrated, lower hydroformylation activities have been commonly observed for inorganic solid catalysts (yellow-shaded area on the plot). Among those, catalysts bearing metal aggregates have faced an activity/selectivity interdependence, wherein activities higher than 20 h^{-1} have been achieved only at the expense of reducing the selectivity to hydroformylation to <80 %. In contrast, recent examples of supported low-nuclearity Rh catalysts, which are marked with the dashed red frame in Fig. 5, have served to showcase Rh-normalized reaction rates >30 h^{-1} concomitantly with hydroformylation selectivity >90 %, e.g. TOF>200 h^{-1} and S_{HF}>95 % for Rh_1/SnO_2 [56]. The latter performance figures contribute to bridging the gap with those

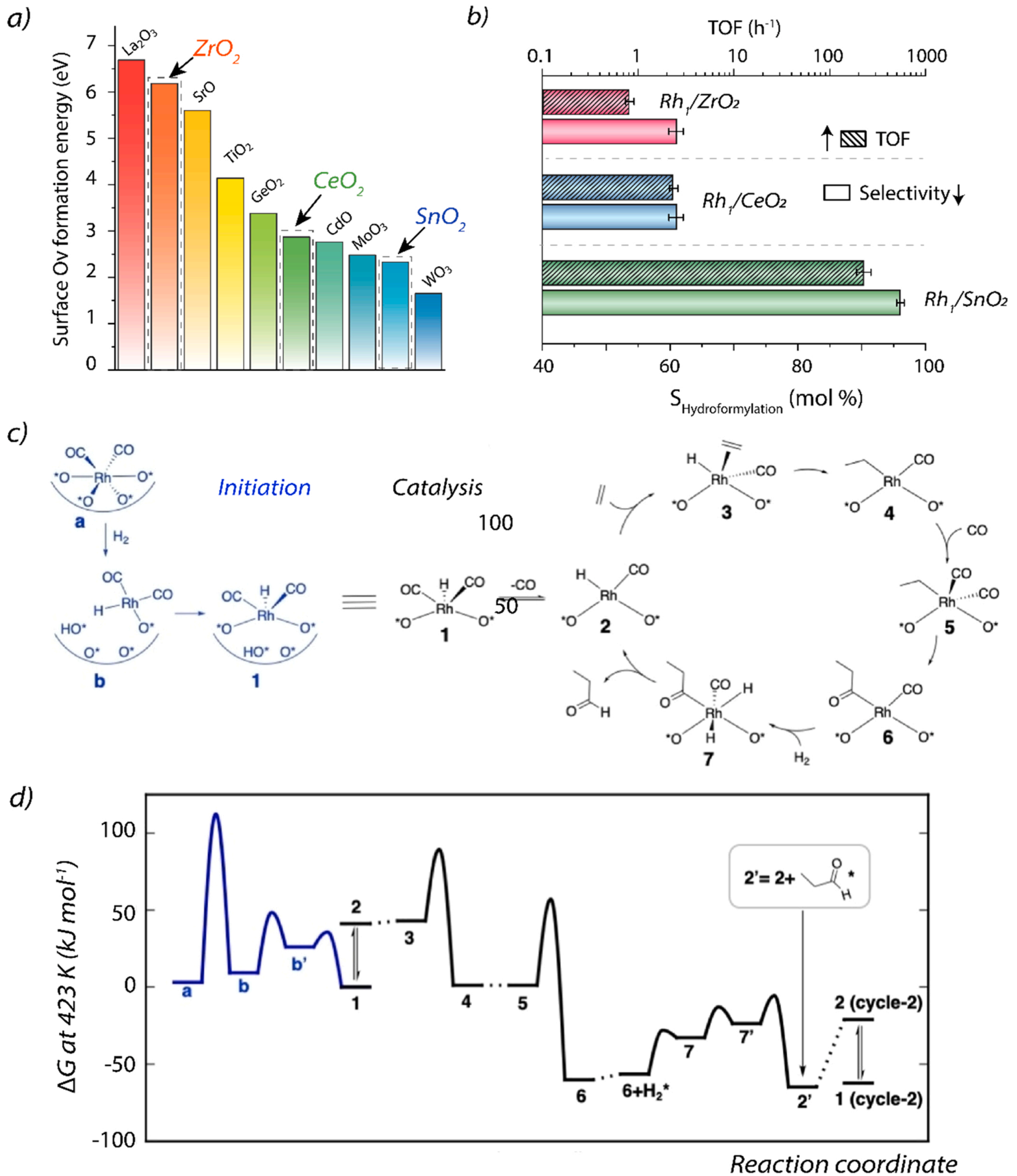

Fig. 4. a) DFT-predicted surface oxygen vacancy (O_v) formation energies for selected metal oxides (no oxygen scavenger consider). b) Initial TOF and hydroformylation selectivity obtained for a series of Rh_1/MO_2 single-atom-catalysts (M=Zr, Ce, Sn) at 423 K and 2.0 MPa. c-d) DFT mechanistic calculations showing: c) the reaction scheme proposed for initiation through the formation of a Rh monohydride dicarbonyl and for the investigated ethylene hydroformylation catalytic cycle and (d) the free energy diagram for the depicted mechanism at T=423 K and P_{CO}=P_{H2}=P_{C2H4} =0.62 MPa reference pressures. Structures resulting from rearrangements or adsorption are not in all cases shown in the scheme and are labeled 7, 7′, etc.
Adapted from [56], copyright (2023), with permission from Wiley-VCH.

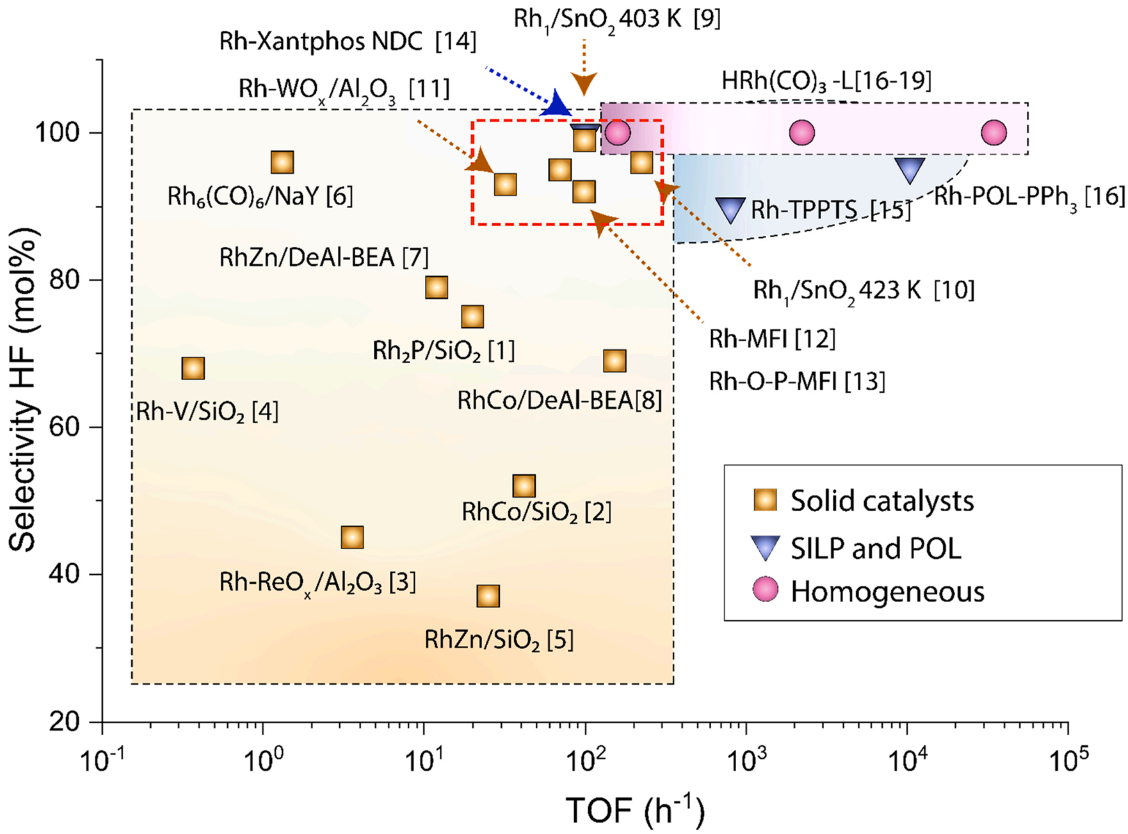

Fig. 5. Comparison of the catalytic performance of different state-of-the-art Rh-based catalysts for gas-phase ethylene hydroformylation, including inorganic solid catalysts (yellow scatter symbols and shaded area), Rh molecular complexes dissolved in the thin liquid film of supported ionic liquid phase (SILP) catalysts or stabilized within a porous organic ligand (POL) (blue scatter symbols and shaded area) and benchmark Rh molecular complexes in solution (pink scatter symbols and shaded area). Recent instances of supported low-atomicity catalysts exhibiting performance akin to that achieved by molecular catalysts are delineated by the dashed red frame. See Table S1 for further details on catalyst composition, reaction conditions and literature references.
Adapted from [56], copyright (2023), with permission from Wiley-VCH.

previously only achievable with molecular coordination complex catalysts, either in solution (region shaded in pink in Fig. 5) or stabilized in an ionic liquid or a porous organic ligand (region shaded in blue).

3.2. Alternative ethylene hydroformylation catalysts based on cobalt and other active metals

Known since the inception of the hydroformylation catalysis, Co-based catalysts constitute the main alternative in olefin hydroformylation processes in general, and ethylene hydroformylation in particular. Already the pioneering work by Roelen and his team revealed the critical need for high P_{CO} (typically corresponding to syngas pressures above 15 MPa) to stabilize active cobalt carbonyl species and avoid the formation of metallic cobalt black. In the 1960s, significant advancements were made with alternative catalyst formulations based on coordination complexes featuring phosphine ligands ($HCo(CO)_3(PR_3)$), where R substituents are typically alkyl or aryl groups. These complexes facilitated electron back-bonding to the metal site, allowing for stable catalysts at lower operational syngas pressures, however, often necessitating higher temperatures around 473 K, which are known to promote secondary reactions like aldehyde and olefin hydrogenation. At present, Co catalysis represents around 20–25 % of the industrialized HF processes, mainly for the hydroformylation of propylene and mid-long chain aliphatic olefins (C_8-C_{16}), being the rest of the oxo-chemicals sector dominated by Rh catalysts [62–64]. While reaction rates with Co-based catalysts can generally not rival those offered by Rh catalysts at milder operation conditions, the high cost and price volatility experienced in recent years by precious metals like Rh, at present ca. 151 USD g^{-1} Rh *vs* 0.03 USD g^{-1} Co, provides impetus for a renaissance of cobalt HF catalysis.

Only few research works have studied solid cobalt catalysts the gas-phase hydroformylation of ethylene. Among those, several studies report bimetallic systems wherein Co acts in combination with Rh or Ru, which casts doubts about the actual catalytic role of cobalt itself [65]. Takeuchi et al. presented in the 1990s one of the few studies using monometallic Co solid catalysts for light olefin hydroformylation [66]. The effect of the metal precursor was addressed on the performance of SiO_2-supported catalysts. The use of $Co_2(CO)_8$ as precursor led to particularly small Co nanoparticles of ca. 1 nm at a total metal surface loading of 1.5 Co_{at} nm^{-2}. The resulting catalyst delivered a Co-specific hydroformylation rate of 5.1 h^{-1} and a total selectivity of 36 % to oxygenates. Navidi et al. studied Al_2O_3-supported Co catalysts. At 473 K and 2.0 MPa, a maximum reaction rate of 13 h^{-1} and a selectivity of 19 % were attained [67]. These performances are significantly poorer than those offered by Rh-based catalysts, particularly those based on single- and few-atom active centers, as discussed above.

Ruthenium is a third active metal increasingly considered in olefin hydroformylation. Albeit less marked than in the case of Co, there are also economic motivations to replace Rh by Ru in HF catalyst formulations, as the current mass-specific market Ru price is ca. 10 times lower than that of Rh. Following the pioneering report by Evans, Osborn, Jardine, and Wilkinson in 1965 [68], numerous Ru-based coordination complex catalysts have been developed. However, as in the case of Co, only few works in the scientific literature have addressed the synthesis of Ru-based solid catalysts for the gas-phase hydroformylation of ethylene. Huang and Xu explored the synthesis of silica-supported Ru catalysts from various metal precursors [69,70]. Despite limited Ru-specific reaction rates of 4–8 h^{-1}, full chemoselectivity was reported, essentially irrespective of the Ru precursor used for catalyst synthesis. Interestingly, when Co was additionally incorporated, hydroformylation activity surged to 30–150 h^{-1}; however, this increase was accompanied by a notable decrease in selectivity to 30 %. No activity was registered with a reference monometallic Co catalyst under the same operating conditions, highlighting the significance of bimetallic synergism.

Although the above catalysts based on alternative metals attain hydroformylation activities comparable to those of supported Rh-based catalysts, chemoselectivity remains a major challenge. This may be tentatively ascribed to the presence of Co and/or Ru metal aggregates, primarily metal nanoparticles with average diameters >1 nm. The exposure of extended metallic surfaces to reactant activation might promote direct olefin hydrogenation. As it shall be discussed below in **Section 4.2** , few studies have reported the stabilization of low-nuclearity Co and Ru as a plausible approach to develop hydroformylation catalysts for propylene and particularly higher olefins [71–73]. Expanding upon these catalyst design strategies is anticipated to improve chemoselectivity in ethylene hydroformylation too.

4. Solid catalysts for propylene hydroformylation

The industrial significance of propylene hydroformylation surpasses that of ethylene. Propylene hydroformylation products, including *1*-butanal (butyraldehyde) and *2*-methylpropanal (isobutyraldehyde), command global markets of approximately 260 and 200 million USD y^{-1}, respectively. These compounds find applications across various sectors, from plasticizer production to the synthesis of synthetic flavors and fragrances, as well as polymer manufacturing, among others. Propylene activation has been reported to be noticeably more difficult to activate than ethylene in the context of hydroformylation catalysis [65, 74]. Mao et al. compared ethylene and propylene hydroformylation reactions on a RhCo/MCM-41 catalyst [65]. Through the combination of catalytic experiments and *in situ* spectroscopy studies, these authors observed that both propylene hydroformylation and hydrogenation rates were about an order of magnitude lower than those registered for ethylene, which they ascribed to a more difficult oxidative addition of propyl (*vs* ethyl) groups to a M-H bond. In addition to differences in the intrinsic reactivity of both olefins, propylene hydroformylation is concerned with product regioselectivity, i.e. the formation of isobutyraldehyde, in line with Markovnikov's regioselectivity rule for acyl additions, or butyraldehyde, following an anti-Markovnikov formyl addition. A regioselective propylene hydroformylation may alleviate downstream separation costs for the two product isomers, which exhibit similar boiling points (348 K vs 337 K at P_{atm}, for the linear (*l*) and branched aldehyde (*b*), respectively).

4.1. Rh-based propylene hydroformylation catalysts

As for ethylene hydroformylation, the application of molecular catalysts dissolved in SILP thin films or stabilized within POP soft matter architectures have been explored as means to heterogenize molecular catalysts while retaining the benefits of a coordination chemistry with well-defined organic ligands. Ding and coworkers proposed the use of Rh/POL catalysts for propylene hydroformylation. Porous ligand matrices were synthesized by the copolymerization of vinyl functionalized biphephos ligands with tris(4-vinphenyl) phosphane and a series of co-ligands [75]. After incorporating Rh as the active metal, the catalysts achieved initial TOF >1200 h^{-1}, coupled with aldehyde selectivities surpassing 93 %. Notably, this was accompanied by a butyraldehyde linear-to-branched (*l*:*b*) molar ratio exceeding 24, indicating >96 % selectivity to butanal within the C_4 aldehyde products. Furthermore, the system demonstrated remarkable stability, maintaining TOF >800 h^{-1} and its chemo/regio-selectivity for over 1000 h of continuous operation. Rh-based SILP catalysts were investigated by Riisager et al.[76,77] A molecular coordination complex of Rh with sulfoxantphos ($C_{39}H_{30}O_7P_2S_2Na$) was dissolved in a thin film of the [BMIM][n-$C_8H_{17}OSO_3$] ionic liquid coated on a SiO_2 carrier. A screening of operational conditions– total and propylene partial pressure, temperature and gas-solid contact time– identified optimal conditions at which a Rh-based TOF >60 h^{-1} was sustained for more than 180 hours on-stream. The system delivered essentially full selectivity to hydroformylation products, with a butyraldehyde *l*:*b* ratio >19 [76].

Rhodium has also been the metal of most frequent choice to develop solid inorganic propylene hydroformylation catalysts. Conventional supported catalysts, i.e. those containing nanocrystals of either neat Rh, Rh-based bimetallics or rhodium phosphide have shown only modest hydroformylation activity, with TOF<5 h^{-1}. Interestingly, chemoselectivity values often exceeded those reported for ethylene hydroformylation, while the butanal *l*:*b* molar ratio was lower than 5 [74,78].

The capacity to stabilize low-nuclearity Rh species on solid matrices provides prospects for better performances. Recently, Zheng et al. synthesized Rh_1/CeO_2 single-atom catalysts [79]. Calcination temperatures >1073 K fostered the formation of oxygen vacancies on the ceria carrier and increased the density of low-coordination Rh sites. The latter species appeared to maximize the rate of propylene hydroformylation in the liquid phase, using *n*-heptane as a solvent. TOF values as high as 5174 h^{-1} were attained, along with full chemoselectivity, indicative for an effective inhibition of propylene hydrogenation. The butyraldehyde *l*:*b* ratio was approximately 1, which is similar to that observed with unmodified Rh carbonyl catalysts in solution [80]. These observations reinforced the existence of an activity/regioselectivity inverse dependence as discussed by Liu et al.[12]

Ligand selection has traditionally been the central design aspect for molecular HF catalysts in the search for high product regioselectivity. Generally, steric hindrance is considered to be the dominant phenomenon steering regioselectivity, although electronic effects on the central Rh atom have also been asserted influential to a certain extent [81]. With solid, inorganic catalysts, however, inducing regioselectivity has long remained a challenge and various strategies have been pursued, as schematically illustrated in Fig. 6.

One of the earliest proposed approaches involves modifying supported Rh nanocrystals through the adsorption of organic ligands. In 2005, Yan et al. modified SiO_2-supported Rh catalysts with triphenylphosphine (PPh_3) and tested the effects of such modification in the gas-phase hydroformylation of propylene [82]. A combination of FTIR, XPS, ^{31}P NMR and thermogravimetric analyses pointed to the development of $HRhCO(PPh_3)_3$ and $HRh(CO)_2(PPh_3)_2$ species on the catalyst surface under reaction conditions, similar to those present in molecular catalysts operating in solution. This system delivered an Rh-specific reaction rate of 230 h^{-1}, together with almost full chemoselectivity (99.5 %) to aldehydes. Moreover, the butyraldehyde *l*:*b* ratio was 8.8, significantly higher than that observed with the unmodified Rh/SiO_2 catalyst (3.1). Few years later, Bell and co-workers adopted a similar catalyst modification strategy, expanded the list of organic ligands/surface modifiers, and studied the influence of reaction conditions [83,84]. These authors observed marked similarities in the optimal ligand:Rh molar ratio with different ligands, suggesting a common promotional principle. Moreover, they confirmed that apparent activation energies for propylene hydroformylation in the gas-phase resembled those previously determined by the same authors with molecular catalysts in liquid media. Butyraldehyde *l*:*b* molar ratios >15 were attained in this case.

A second strategy relies on the engineering of low-nuclearity metal centers. Wang et al. observed a 94.4 % regioselectivity to butanal, i.e. corresponding to a butyraldehyde *l*:*b* ratio of 17, in the liquid-phase hydroformylation of propylene on atomically dispersed Rh_1/CoO solid catalysts, using *2*-propanol as solvent [85]. Remarkably, this anti-Markovnikov regioselectivity was attained in conjunction with high hydroformylation activity (TOF=2065 h^{-1}) at 373 K. Based on periodic DFT mechanistic calculations, the authors attributed the unconventionally high regioselectivity to a limited number of adsorption

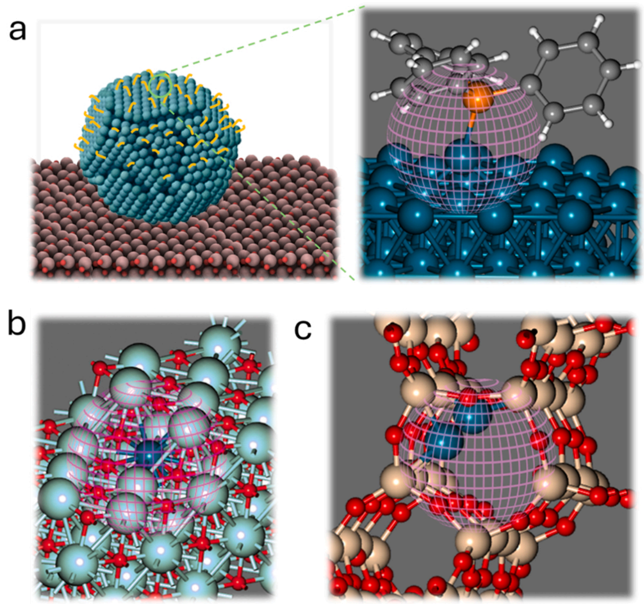

Fig. 6. Schematic illustration of strategies proposed for steering regioselectivity with Rh-based solid catalysts in the hydroformylation of propylene: a) surface modification of supported metal nanoparticles with organic ligands (triphenyl phosphine shown as an example); b) partial confinement of isolated Rh sites within the surface of metal oxide supports in single-atom catalysts; and c) confinement of Rh active sites (a Rh_2 cluster shown as an example) within zeolite channels of molecular dimensions. In the figures the netted sphere illustrates the direct coordination sphere of the Rh centers, which is believed to induce steric effects on propylene activation and affect hydroformylation product regioselectivity.

configurations on the Rh center partially confined to the lattice of CoO. As illustrated in Fig. 7, reactant co-adsorption configurations which favor a terminal CO insertion, and thus a terminal butyraldehyde product, were found to be ca. 0.06 eV (ca. 6 kJ mol^{-1}) more stable than those eventually leading to a Markovnikov hydroformylation. While this energy difference is typically within the accuracy of periodic DFT calculations at the applied theory level (DFT+U, PAW-PBE) it was considered by the authors to be sufficient to steer the reaction mechanism preferentially towards the formation of the linear aldehyde product.

A third approach successfully demonstrated to control regioselectivity is the exploitation of electrostatic and dispersive forces in nanoconfined reaction spaces, such as those provided by microporous molecular sieves. Molecular-sized void spaces in zeotype materials, i.e. channels and cavities of molecular dimensions, are known to contribute to stabilizing even un-charged reaction transition states and intermediates through dispersion forces, thereby influencing the dynamics of elementary conversion steps along reaction mechanisms [86–88]. Conceptually, this working principle has been associated to that at play in enzymatic catalysis, wherein biocatalysts feature active centers within pockets decorated by specific amino acid residues, which are central to stabilize substrates and transition states, predominantly through non-covalent interactions. With inorganic zeolite catalysts, these effects have been long proposed to underlie shape selectivity in reactions occurring on Bronsted acid centers associated to the zeolitic silicoaluminate frameworks [89,90]. Extending such host-induced shape selectivity to metal catalysis, through the encapsulation of low-atomicity metal species within the microporous architecture of zeotype materials, has been a matter of research over the last years.

Zhang et al. proposed the use of K-doped Rh clusters, entrapped within the microporous structure of silicalite-1 zeolite (MFI), as catalysts for the hydroformylation of propylene in liquid phase, using toluene as solvent [91]. These authors observed a profound impact of K-doping on catalytic performance, identifying an optimum K:Rh molar ratio of 20, for which a maximum hydroformylation activity, corresponding to TOF=7328 h^{-1}, was attained at 358 K and 5.0 MPa total pressure (Fig. 8). Moreover, this activity was accompanied by a butyraldehyde *l:b* molar ratio of about 5 (83 % abundance of butanal in the C_4 aldehyde products). This performance was ascribed to the capacity of the K cations to modify Rh clusters in the confinement of the zeolite host, both electronically as well as sterically, favoring a terminal adsorption configuration of propylene on the metal active centers. Interestingly, the same catalyst delivered much lower reaction rates (2.5 h^{-1}) when the process was performed in the gas-phase, using a packed-bed reactor at 412 K and 1.0 MPa. While no regioselectivity data were reported in the latter case, the dramatic change in hydroformylation activity suggests an important role of the solvent and/or propylene partial pressure for performance.

In a recent study, Zhang et al. achieved the encapsulation of few-atom Rh clusters and isolated atoms within the micropore architecture of medium-pore zeolite MEL using a one-pot synthesis approach. This method involved the incorporation of an ethylenediamine Rh(III) complex into the zeolite crystallization gel [92]. These catalysts were tested for the hydroformylation of propylene in liquid phase, using toluene as solvent. Moreover, these authors demonstrated the addition of *2, 4*-dimethylbenzenethiol (DMBT) to the reaction media as an ingenious approach to selectively poison Rh sites which may have remained accessible on the outer surface of the zeolite crystals (Fig. 9). Rh sites in the confinement of the micropores remained intact, as the bulky DMBT molecule cannot access intracrystalline void spaces. At 363 K and a total pressure of 4.0 MPa (H_2:CO:propylene:Ar 47:47:2:4) these catalysts exhibited a remarkably high hydroformylation TOF of ca. 6500 h^{-1}. Most notably, this activity was combined with an impressive regioselectivity to butanal, corresponding to butyraldehyde *l:b* molar ratios >100. The role of DMBT to restrict activity to the inner space of the zeolite crystals, by inhibiting insufficiently unconfined Rh sites, was demonstrated by the observation of a much lower butyraldehyde *l:b* ratio of 4.9 in the absence of this thiol poison. Periodic DFT calculations (using PAW-PBE-D3) indicated that CO insertion into the Rh-propyl bond is the rate-determining step. Furthermore, these calculations revealed an approximately 0.43 eV higher energy barrier for this step in the mechanism leading to the branched *2*-methylpropanal product. This implies that dispersive force interactions with framework oxygen atoms in the zeolite stabilize the transition state along the alternative reaction path leading to linear butanal, driving the remarkable regioselectivity observed.

Fig. 10 provides an overview of state-of-the-art solid Rh catalysts for propylene hydroformylation. See Table S2 in the Supporting Information for additional details. Different catalyst systems are organized on the basis of three performance indicators, i.e. Rh-specific hydroformylation rate (corresponding to TOF in those cases wherein all Rh atoms are considered to act as active centers), chemoselectivity to aldehydes and regioselectivity, captured by the butyraldehyde *l:b* molar ratio in the products. As illustrated on the plot (yellow scatter symbols), conventional supported catalysts bearing Rh in nanoparticulate form have shown only moderate activities (<4 h^{-1}) and regioselectivity, with *l:b*=1–5. A substantial improvement in performance has been attained by modifying Rh nanoparticles with phosphine organic ligands/adsorbates (pink data points on the plot), reaching reaction rates >200 h^{-1} with excellent chemoselectivity >99.5 % and notably enhanced butyraldehyde *l:b* ratio in the range of 9–15. As discussed above, the stabilization of low-atomicity Rh species, i.e. few-atom clusters and single atoms, has proven a successful strategy to dramatically enhance propylene hydroformylation rates by more than an order to magnitude, up to >7000 h^{-1} while simultaneously achieving essentially full chemoselectivity, through the effective inhibition of propylene hydrogenation (see green symbols on the graph). For the latter type of supported catalysts, further exploitation of confinement and shape-selectivity effects within zeotype hosts has recently enabled essentially full

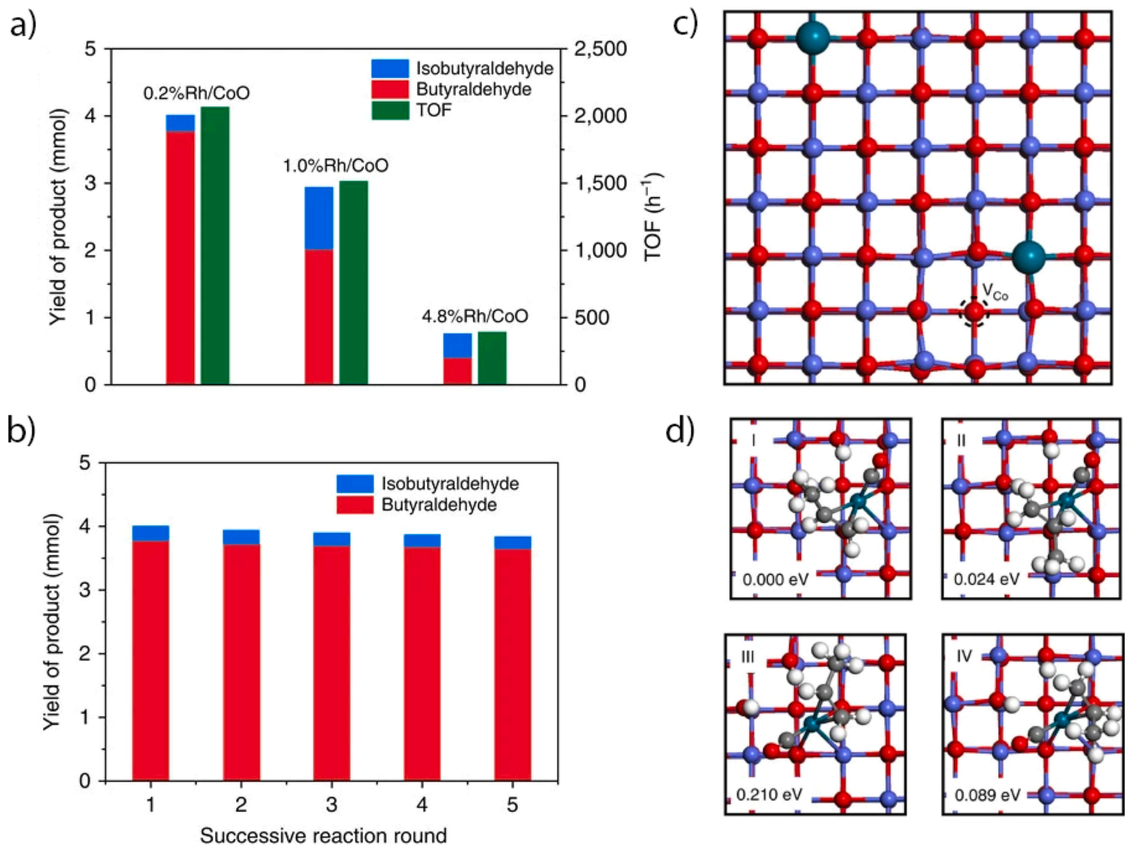

Fig. 7. Catalytic performance results showing a) TOF and product yields obtained with 0.2 %Rh/CoO, 1.0 %Rh/CoO, and 4.8 %Rh/CoO catalysts in the hydroformylation of propylene at 273 K after 2 h and b) product yield over consecutive catalyst recycling tests with 0.2 %Rh/CoO at 273 K. c,d) DFT calculations on a Rh_1/CoO propylene hydroformylation catalyst. c) Structural model for the atomically dispersed catalyst. d) Four different co-adsorption configurations for hydroformylation reactants and their corresponding total energies, relative to most stable configuration I.
Adapted from reference [85], copyright (2016), with permission from Nature Springer.

regioselectivity to the linear butyraldehyde product (*l*:*b*>100). This evidence renders low-atomicity supported Rh catalysts the most promising class of inorganic catalyst alternative to approach those performances typically offered by classical homogeneous catalysis systems. As illustrated in Fig. 10 (red scatter symbols), the latter typically attain turnover frequencies in the range of 900–9000 h^{-1}, chemoselectivity values >98 % and butyraldehyde *l*:*b* ratios in the range of 13–50.

It is noteworthy that propylene hydroformylation experiments with solid catalysts have been conducted using a slurry-type reactor with a solvent in some studies, while in other instances, continuous gas-solid operations have been demonstrated in packed-bed reactors. Only in a limited number of works have both reaction conditions been comparatively assessed, revealing remarkable differences in performance for the same catalyst. Solvent media often do not play an innocent role in catalysis. For supported solid catalysts, they may provide additional “ligation” effects on the metal active centers or facilitate product desorption via solvation phenomena. In the case of catalytic metal species encapsulated within molecular sieve hosts, the effective molecular size of the solvent molecules may determine whether the latter infiltrates the pore system of the catalyst and, therefore, the nature of the direct environment around the metal active centers under reaction conditions. Further research is needed to fully rationalize these phenomena and progress to optimal hydroformylation performance and catalyst stability under the preferred continuous gas-solid operation settings.

4.2. Alternative propylene hydroformylation catalysts based on cobalt and other active metals

For reasons discussed above, the pursuit of alternative hydroformylation active metals to replace Rh represents a highly appealing research area. Similarly to the case of ethylene, only a limited number of literature studies have addressed alternative metals for propylene hydroformylation. This likely stems from the fact that propylene is intrinsically difficult to activate under reaction conditions mild enough to prevent side-hydrogenation to propane, and Rh has proven to be the most effective metal to attain hydroformylation activity under mild operation settings.

Few studies have considered Co-based catalysts. In the 1970s, Ichiwaka [74] studied series of Rh and Co-based solid catalysts supported on different metal oxides. Under gas-phase propylene hydroformylation conditions, a Co/ZnO catalyst synthesized by deposition of $Co_4(CO)_{12}$ on ZnO, followed by thermal decomposition of the metal carbonyl precursor, offered full chemoselectivity with a butyraldehyde *l*:*b* ratio of 9. However, this selectivity was accompanied by a notoriously low Co-specific reaction rate of 0.12 h^{-1}. In a more recent work, Wei et al. developed a Co catalyst atomically dispersed on b-Mo_2C, which showed Rh-like performance, i.e. a Co-based TOF of ca. 750 h^{-1} alongside 90 % selectivity, and a butyraldehyde *l*:*b* ratio of 1 [93]. Electronic modulation exerted by the molybdenum carbide on the isolated Co sites was posited to explain this unconventional performance. Also gold, which is conventionally not considered as a relevant active metal in HF catalysis has been studied. Wei et al. reported that, while Au aggregates (nanoclusters and nanoparticles) show the inefficiency which is presumed for this metal, cationic gold atoms isolated within the inner micropore

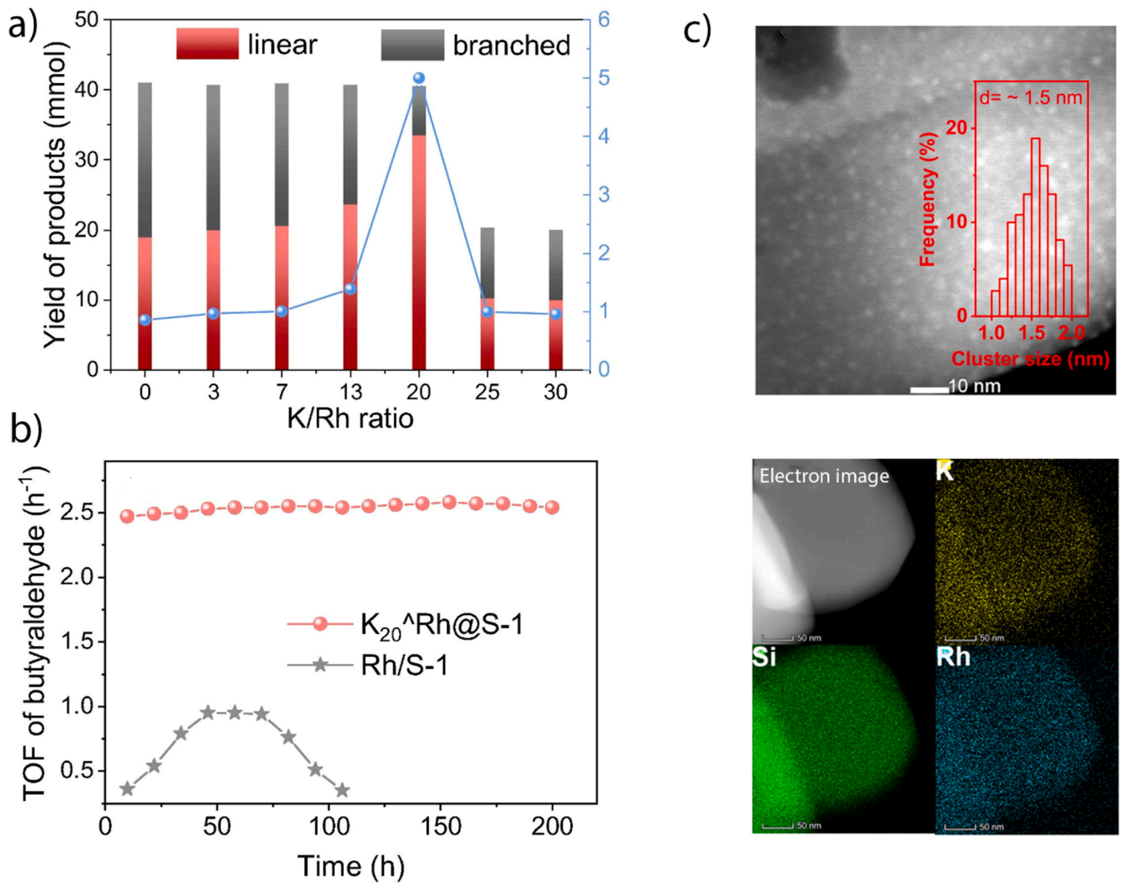

Fig. 8. a) Product yield for the hydroformylation of propylene with $\hat{K}_x$Rh@S-1 catalysts, as a function of the molar K:Rh ratio. Reaction conditions: catalyst (0.1 g, Rh = 0.2 wt%), propylene (0.5 MPa), CO:H_2 = 1:1 (5 MPa), toluene (5 mL), 358 K, 3 h. b) Stability assessment for the gas-phase hydroformylation of propylene $\hat{K}_{20}$Rh@S-1. Reaction conditions: Catalyst 3 g, propylene:CO:H_2 = 1:1:1, 1 MPa, 15 mL min^{-1}, 413 K. c) HAADF-STEM micrographs and the corresponding EDS elemental mappings for $\hat{K}_{20}$Rh@S-1. The inset to the STEM micrograph shows the Rh cluster size distribution.
Adapted from [91], copyright (2020), with permission from Elsevier.

network of the silicalite-1 (MFI) zeolite deliver propylene hydroformylation activity [94].

5. Conclusions and perspectives

The design of solid catalysts for selective olefin hydroformylation has made significant strides in recent years, motivated by the technical and economic benefits anticipated in replacing state-of-the-art homogeneous catalysis technologies. There has been notable emphasis on designing catalysts for ethylene and propylene hydroformylation, which collectively represent over 70 % of the current oxo-chemicals market. The development of light-olefin hydroformylation processes offers avenues for simplified catalyst recovery, diminished or circumvented precious metal losses, and enables continuous operation.

Beyond yielding higher added-value C_{3-4} aldehyde and alcohol chemicals, the (reductive) hydroformylation of light olefins may provide the basis for a reactive separation to recover ethylene and propylene from diluted gas streams containing low-value alkanes. Our preliminary techno-economic assessment exemplifies this by comparing a conventional, cryogenic distillation ethylene/ethane splitter with a reactive separation using selective ethylene reductive hydroformylation to *1*-propanol. Evaluation of utility costs revealed significant savings for the latter process.

Research efforts have been particularly concentrated on designing solid catalysts for ethylene hydroformylation, aiming to tackle the challenges posed by the high reactivity of this C_2 olefin and the pronounced thermodynamic preference for olefin hydrogenation side reactions. Strategies for heterogenizing hydroformylation (HF) catalysts have sought to mimic the structure and performance of conventional molecular complexes used in free form or solution. Innovative approaches, such as Supported Ionic Liquid Phase (SILP) and Porous Organic Ligands (POLs), have demonstrated remarkable performance in gas-phase ethylene hydroformylation. However, the development of fully inorganic catalysts holds greater appeal due to their easier handling, superior stability, and lower cost.

Among the reported approaches, utilizing low-nuclearity metal sites, such as single-atom catalysts (SACs) and sub-nanometer clusters, dispersed on suitable supports like metal oxides with carefully selected redox properties or within the microporous architecture of certain zeolites, has recently led to breakthroughs. These advancements have achieved ethylene hydroformylation performances previously only attainable with molecular catalysts. In propylene hydroformylation, achieving control over regioselectivity introduces additional complexity. Recent research has shown that stabilizing isolated metal atoms and clusters within molecular-sized environments, such as zeolitic channels, is an effective strategy. This approach has demonstrated high activity, as well as chemo- and regioselectivity, occasionally outperforming benchmark molecular catalysts.

In spite of the significant achievements discussed here, further research is needed in the field to gain a deeper understanding of certain aspects. This includes exploring the role of solvents in slurry-phase hydroformylation processes. Solvents are generally considered crucial in catalytic processes, and assessing their contribution to reaction rates poses a complex problem due to various potentially involved

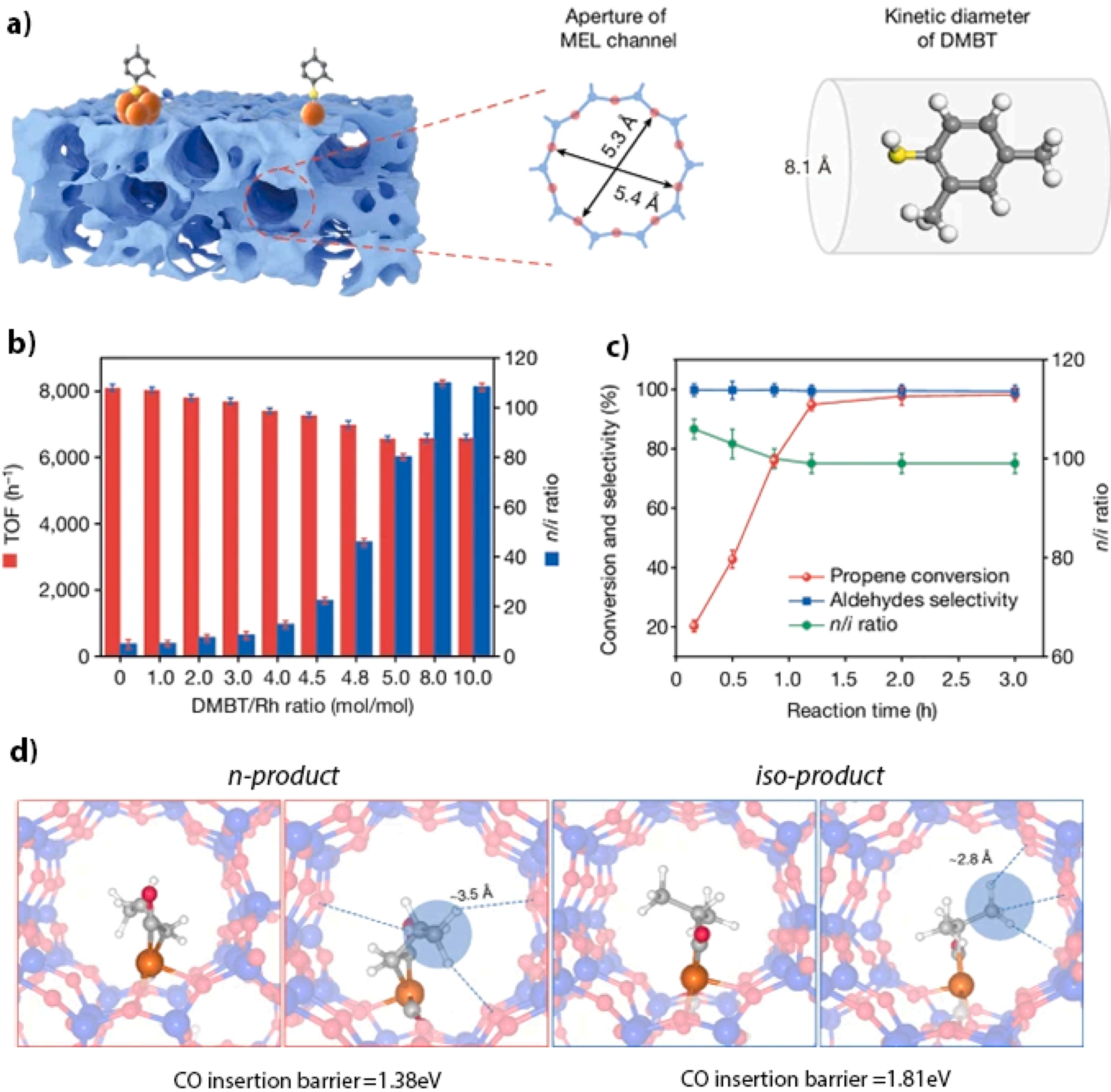

Fig. 9. a) Schematics of the selective inhibition of unconfined Rh sites on the outer surface of the zeolite crystals by chemisorption of *2,4*-dimethylbenzenethiol (DMBT). b) Evolution of the propylene hydroformylation turnover frequency (TOF), determined per unit total Rh atoms, and the butyraldehyde product regioselectivity as a function of the DMBT concentration for 0.17RhOD@MEL-catalysed propylene hydroformylation. Reaction conditions: 20 mg of catalyst, 4 mL of toluene, 4 MPa of H_2/CO/propylene/Ar (47:47:2:4, vol), 363 K, 30 min. c) Dependence of propylene conversion and (regio)selectivity with the reaction time over the DMBT-selectivated 0.17RhOD@MEL catalyst. d) Representations of the DFT-identified transition states for the CO insertion mechanistic step along the formation pathways for *n*- and *iso*-aldehyde products, showing predicted distances to zeolite framework oxygen anions.
Adapted from [92], copyright (2024), with permission from Springer Nature.

phenomena. These include alterations in reagent solubility and/or mass transfer coefficients, thermodynamic non-idealities, competitive adsorption with substrate molecules for active sites, and the stabilization of transition states for reaction/desorption elementary kinetic steps through solvation phenomena [95]. The level of complexity becomes even more pronounced in meso- and particularly microporous solid catalysts, where capillarity and steric exclusion effects may arise, further altering the packing, mobility, and thus the action of solvent molecules in the confinement of pores [96]. In the current literature, only a few studies have methodically compared the performance of solid catalysts in gas- and slurry-phase processes, typically indicating a decline in catalytic performance under solvent-free operation. Therefore, there remains a knowledge gap that necessitates systematic studies to assess the role of solvents, especially as a function of the structural properties of the solid catalyst. Such studies would ideally facilitate a rigorous assessment of solvation and mass transfer effects on heterogeneous hydroformylation catalysis.

The use of solvents in liquid-phase processes exacerbates the issue of metal leaching. Under hydroformylation conditions, the high CO fugacity typically promotes the formation of labile metal polycarbonyl

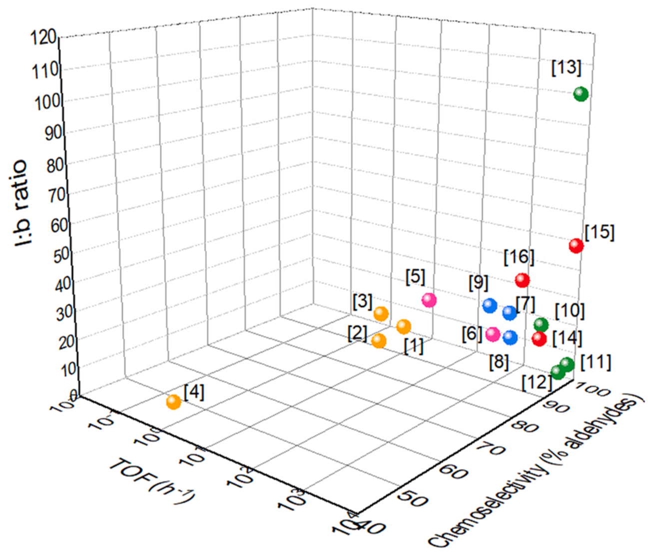

Fig. 10. Comparison of the catalytic performance of different state-of-the-art Rh-based catalysts for propylene hydroformylation. The plot includes conventional solid catalysts (yellow points), phosphine-modified supported catalysts (pink points), Rh molecular complexes dissolved in the thin liquid film of supported ionic liquid phase (SILP) catalysts or stabilized within porous organic ligand (POL) frameworks (blue points), promising single-atom and sub-nanometric cluster-based Rh oxide/zeolite supported catalysts (green points) and benchmark Rh molecular catalysts in solution (red points). See Table S2 for further details on catalyst composition, reaction conditions and literature references.

species. Depending on the reaction conditions, these species may mediate reductive metal agglomeration processes into larger and more stable metal aggregates or leave the catalyst surface, leading to undesired metal losses and product contamination. On the contrary, a high olefin fugacity has been reported to have a positive impact on catalyst stability, by suppressing Rh agglomeration and leaching. This effect has been ascribed to the competitive adsorption of the olefin substrate on supported Rh sites, hindering excessive metal reduction into labile Rh polycarbonyl complexes [97]. Leaching becomes particularly of concern with low-nuclearity metal catalysts, which expose more reactive species to ligand molecules. In gas-solid processes, the finite vapor pressure of metal polycarbonyl compounds[98] may result in permanent desorption of active metal and its entrainment with the gas flow. However, leaching is generally believed to be favored by the extra stabilization provided by coordination ligands or dispersive forces with solvent molecules in liquid media. Given that a minority of dissolved species may significantly influence the overall hydroformylation performance, overlooking or improperly assessing leaching could severely undermine the establishment of reliable catalyst structure-performance relationships. Solid catalysts can maintain recyclability, even when they serve solely as a source of active species in solution, at very low concentrations (ppb/ppm) during each reaction run. Conducting dedicated tests, such as hot-filtration experiments followed by assessing reactivity in reaction liquors, is generally recommended to ascertain the heterogenous nature of the catalysis. While the practice of hot-filtration experiments appears to be declining in current research practices, it is crucial to uphold rigorous experimental protocols to minimize the risk of overlooking metal leaching phenomena and ensure accurate identification of the true active species. This is particularly essential in slurry-phase hydroformylation catalysis, where metal, e.g. Rh, Co, Ru polycarbonyl coordination compounds exhibit both significant solubility and hydroformylation reactivity.

Another critical aspect closely linked to identifying active species and establishing catalyst structure-performance relationships with solid catalysts is site heterogeneity. Synthesis routes aimed at stabilizing low-nuclearity metal species on solid carriers can result in a variety of species, varying in their nuclearity, such as mixtures of single atoms and metal nanoclusters, or differing in their direct chemical environments. Once again, even a small fraction of supported metal centers can significantly influence macroscopically observed catalytic performance. Moreover, these metastable species may exhibit particularly strong dynamics under reaction conditions, complicating the task of identifying the true active sites. Therefore, the application of *operando* characterization methods, which interrogate the catalyst (nano)structure while exposed to high CO, H_2, and olefin partial pressures and, where relevant, also solvent conditions pertinent to hydroformylation catalysis, along with systematic investigations using model catalysts displaying well-defined active centers, is virtually essential for rigorously identifying and rationally maximizing the active centers in solid catalysts. For hydroformylation-relevant metals like Rh and Ru, which form particularly stable polycarbonyl coordination complexes, CO-driven oxidative cluster/crystallite disruption[99,100] and adatom migration/aggregation[101,102] phenomena need to be carefully considered. Changes in aggregation state, e.g. switching between isolated supported metal complexes and clusters may proceed reversibly, as demonstrated for Rh and other transition metals within zeolites and on metal oxide carriers [103,104]. These processes are strongly influenced by factors such as the starting metal aggregation state, temperature, and the composition of the surrounding gas atmosphere, which in the specific case of hydroformylation catalysis dictates CO and olefin surface coverages on the active sites. They may emerge as part of the catalyst dynamics and could potentially obscure site identification if catalyst characterization conditions depart from those of significance for catalyst usage.

CRediT authorship contribution statement

Marcos G. Farpón: Writing – original draft, Methodology, Investigation, Conceptualization. **Gonzalo Prieto:** Writing – review & editing, Supervision, Project administration, Funding acquisition, Conceptualization.

Declaration of Competing Interest

The authors declare that they have no known competing financial interests or personal relationships that could have appeared to influence the work reported in this paper.

Data availability

Data will be made available on request.

Acknowledgements

This work has received funding from the European Research Council (ERC-CoG, TANDEng, Grant Agreement Nr. 864195). Parts of this work have received support by the Spanish Ministry of Science and Innovation, through grants CEX2021-001230-S and PID2022-140111OB-I00, funded by MCIN/AEI/10.13039/501100011033. M.G.F acknowledges support by the Ministry of Education of Spain through his predoctoral grant FPU17/04701. J. Prieto is acknowledged for his contributions to artwork design.

Appendix A. Supporting information

Supplementary data associated with this article can be found in the online version at doi:10.1016/j.cattod.2024.115052.

References

[1] O. Roelen, Verfahren zur Herstellung von sauerstoffhaltigen Verbindungen, DE849548C, 1938.
[2] R. Franke, D. Selent, A. Börner, Applied Hydroformylation, Chem. Rev. 112 (2012) 5675–5732, https://doi.org/10.1021/cr3001803.
[3] K.-D. Wiese, D. Obst, in: M. Beller (Ed.), Hydroformylation BT - Catalytic Carbonylation Reactions, Springer Berlin Heidelberg, Berlin, Heidelberg, 2006, pp. 1–33, https://doi.org/10.1007/3418_015.
[4] B. Zhang, D. Peña Fuentes, A. Börner, Hydroformylation, ChemTexts 8 (2021) 2, https://doi.org/10.1007/s40828-021-00154-x.
[5] V.A. Likholobov, B.L. Moroz, Hydroformylation on solid catalysts. Handb. Heterog. Catal., Wiley, 2008, pp. 3663–3684, https://doi.org/10.1002/9783527610044.hetcat0189.
[6] G.D. Frey, 75 Years of oxo synthesis – the success story of a discovery at the OXEA Site Ruhrchemie, J. Organomet. Chem. 754 (2014) 5–7, https://doi.org/10.1016/j.jorganchem.2013.12.023.
[7] S. Hanf, L. Alvarado Rupflin, R. Gläser, S.A. Schunk, Current state of the art of the solid Rh-based catalyzed hydroformylation of short-chain olefins, Catal 10 (2020), https://doi.org/10.3390/catal10050510.
[8] S.S. Nurttila, P.R. Linnebank, T. Krachko, J.N.H. Reek, Supramolecular approaches to control activity and selectivity in hydroformylation catalysis, ACS Catal. 8 (2018) 3469–3488, https://doi.org/10.1021/acscatal.8b00288.
[9] M. Beller, B. Cornils, C.D. Frohning, C.W. Kohlpaintner, Progress in hydroformylation and carbonylation, J. Mol. Catal. A Chem. 104 (1995) 17–85, https://doi.org/10.1016/1381-1169(95)00130-1.
[10] W.L. Peddie, Separation of homogeneous hydroformylation catalysts using Organic Solvent Nanofiltration, Stellenbosch University, 2016.
[11] B. Liu, N. Huang, Y. Wang, X. Lan, T. Wang, Promotion of inorganic phosphorus on Rh catalysts in styrene hydroformylation: geometric and electronic effects, ACS Catal. 11 (2021) 1787–1796, https://doi.org/10.1021/acscatal.0c04684.
[12] B. Liu, Y. Wang, N. Huang, X. Lan, Z. Xie, J.G. Chen, T. Wang, Heterogeneous hydroformylation of alkenes by Rh-based catalysts, Chem 8 (2022) 2630–2658, https://doi.org/10.1016/j.chempr.2022.07.020.
[13] N. Huang, B. Liu, X. Lan, B. Yan, T. Wang, Promotion of diphosphine ligands (PPh2(CH2) PPh2, n = 1, 2, 3, 5, 6) for supported Rh/SiO2 catalysts in heterogeneous ethene hydroformylation, Mol. Catal. 511 (2021) 111736, https://doi.org/10.1016/j.mcat.2021.111736.
[14] J.L. Vidal, W.E. Walker, Rhodium carbonyl cluster chemistry under high pressure of carbon monoxide and hydrogen. 3. Synthesis, characterization, and reactivity of HRh(CO)4, Inorg. Chem. 20 (1981) 249–254, https://doi.org/10.1021/ic50215a049.
[15] Johnson Matthey, PGM management: Rh price, (2023).
[16] Trading Economics, Commodity (Rh) Price, (2023).
[17] S.K. Kaiser, Z. Chen, D. Faust Akl, S. Mitchell, J. Pérez-Ramírez, Single-atom catalysts across the periodic table, Chem. Rev. 120 (2020) 11703–11809, https://doi.org/10.1021/acs.chemrev.0c00576.
[18] B. Qiao, A. Wang, X. Yang, L.F. Allard, Z. Jiang, Y. Cui, J. Liu, J. Li, T. Zhang, Single-atom catalysis of CO oxidation using Pt1/FeOx, Nat. Chem. 3 (2011) 634–641, https://doi.org/10.1038/nchem.1095.
[19] M. Flytzani-Stephanopoulos, B.C. Gates, Atomically dispersed supported metal catalysts, Annu. Rev. Chem. Biomol. Eng. 3 (2012) 545–574, https://doi.org/10.1146/annurev-chembioeng-062011-080939.
[20] H. Zimmermann, R. Walzl, Ethylene. Ullmann's Encycl. Ind. Chem., Wiley-VCH Verlag GmbH & Co. KGaA, Weinheim, Germany, 2009, https://doi.org/10.1002/14356007.a10_045.pub3.
[21] A. Corma, E. Corresa, Y. Mathieu, L. Sauvanaud, S. Al-Bogami, M.S. Al-Ghrami, A. Bourane, Crude oil to chemicals: light olefins from crude oil, Catal. Sci. Technol. 7 (2017) 12–46, https://doi.org/10.1039/C6CY01886F.
[22] D.N. Gorbunov, M.V. Terenina, Y.S. Kardasheva, A.L. Maksimov, E. A. Karakhanov, Oxo processes involving ethylene (a Review), Pet. Chem. 57 (2017) 1137–1140, https://doi.org/10.1134/S0965544117060159.
[23] W.J. Tenn, R.C. Singley, B.R. Rodriguez, J.C. DellaMea, Reactive separation of dilute ethylene by hydroformylation using slurried rhodium catalysts on phosphinated resins and silica, Catal. Commun. 12 (2011) 1323–1327, https://doi.org/10.1016/j.catcom.2011.05.001.
[24] D.S. Sholl, R.P. Lively, Seven chemical separations to change the world, Nature 532 (2016) 435–437, https://doi.org/10.1038/532435a.
[25] D. Saha, B. Toof, R. Krishna, G. Orkoulas, P. Gismondi, R. Thorpe, M.L. Comroe, Separation of ethane-ethylene and propane-propylene by Ag(I) doped and sulfurized microporous carbon, Microporous Mesoporous Mater. 299 (2020) 110099, https://doi.org/10.1016/j.micromeso.2020.110099.
[26] J.-W. Yoon, I.-T. Jang, K.-Y. Lee, Y.-K. Hwang, J.-S. Chang, Adsorptive separation of propylene and propane on a porous metal-organic framework, copper trimesate, Bull. Korean Chem. Soc. 31 (2010) 220–223, https://doi.org/10.5012/bkcs.2010.31.01.220.
[27] D. Banerjee, J. Liu, P.K. Thallapally, Separation of C 2 hydrocarbons by porous materials: metal organic frameworks as platform, Comments Inorg. Chem. 35 (2015) 18–38, https://doi.org/10.1080/02603594.2014.976704.
[28] F.G. Kerry, Industrial Gas Handbook: Gas Separation and Purification, CRC press, 2007.
[29] R.B. Eldridge, Olefin/paraffin separation technology: a review, Ind. Eng. Chem. Res. 32 (1993) 2208–2212, https://doi.org/10.1021/ie00022a002.
[30] R. Wei, X. Liu, Z. Lai, MOF or COF membranes for olefin/paraffin separation: Current status and future research directions, Adv. Membr. 2 (2022), https://doi.org/10.1016/j.advmem.2022.100035.
[31] T. Rösler, K.R. Ehmann, K. Köhnke, M. Leutzsch, N. Wessel, A.J. Vorholt, W. Leitner, Reductive hydroformylation with a selective and highly active rhodium amine system, J. Catal. 400 (2021) 234–243, https://doi.org/10.1016/j.jcat.2021.06.001.
[32] F.M.S. Rodrigues, P.K. Kucmierczyk, M. Pineiro, R. Jackstell, R. Franke, M. M. Pereira, M. Beller, Dual Rh−Ru catalysts for reductive hydroformylation of olefins to alcohols, ChemSusChem 11 (2018) 2310–2314, https://doi.org/10.1002/cssc.201800488.
[33] M.B. Leo, A. Dutta, S. Farooq, Process synthesis and optimization of heat pump assisted distillation for ethylene-ethane separation, Ind. Eng. Chem. Res. 57 (2018) 11747–11756, https://doi.org/10.1021/acs.iecr.8b02496.
[34] M. Mafi, S.M.M. Naeynian, M. Amidpour, Exergy analysis of multistage cascade low temperature refrigeration systems used in olefin plants, Int. J. Refrig. 32 (2009) 279–294, https://doi.org/10.1016/j.ijrefrig.2008.05.008.
[35] H. Wang, P. Yu, L. Chen, L. Chen, B. Sun, Simulation and modification of an Ethane-Ethylene separation Unit using vapor recompression heat Pump: energy, Exergy, and economic analyses, Appl. Therm. Eng. 239 (2024) 121993, https://doi.org/10.1016/j.applthermaleng.2023.121993.
[36] S. Pandey, G.P. Rangaiah, Multiobjective Optimization of Cold-End Separation Process in an Ethylene Plant, Ind. Eng. Chem. Res. 52 (2013) 17229–17240, https://doi.org/10.1021/ie4027764.
[37] M.G. Farpón, W. Henao, P.N. Plessow, E. Andrés, R. Arenal, C. Marini, G. Agostini, F. Studt, G. Prieto, Rhodium single-atom catalyst design through oxide support modulation for selective gas-phase ethylene hydroformylation, Angew. Chem. Int. Ed. n/a (2022) e202214048, https://doi.org/10.1002/anie.202214048.
[38] J.M. Marinkovic, A. Riisager, R. Franke, P. Wasserscheid, M. Haumann, Fifteen years of supported ionic liquid phase-catalyzed hydroformylation: material and process developments, Ind. Eng. Chem. Res. 58 (2019) 2409–2420, https://doi.org/10.1021/acs.iecr.8b04010.
[39] M.T. Heinze, J.C. Zill, J. Matysik, W.D. Einicke, R. Gläser, A. Stark, Solid–ionic liquid interfaces: pore filling revisited, Phys. Chem. Chem. Phys. 16 (2014) 24359–24372, https://doi.org/10.1039/C4CP02749C.
[40] M. Haumann, A. Riisager, Hydroformylation in room temperature ionic liquids (RTILs): catalyst and process developments, Chem. Rev. 108 (2008) 1474–1497, https://doi.org/10.1021/cr078374z.
[41] Y. Chauvin, L. Mussmann, H. Olivier, A novel class of versatile solvents for two-phase catalysis: hydrogenation, isomerization, and hydroformylation of alkenes catalyzed by rhodium complexes in liquid 1,3-dialkylimidazolium salts, Angew. Chem. Int. Ed. Engl. 34 (1996) 2698–2700, https://doi.org/10.1002/anie.199526981.
[42] A. Weiß, M. Giese, M. Lijewski, R. Franke, P. Wasserscheid, M. Haumann, Modification of nitrogen doped carbon for SILP catalyzed hydroformylation of ethylene, Catal. Sci. Technol. 7 (2017) 5562–5571, https://doi.org/10.1039/C7CY01346A.
[43] H.N.T. Ha, D.T. Duc, T.V. Dao, M.T. Le, A. Riisager, R. Fehrmann, Characterization and parametrical study of Rh-TPPTS supported ionic liquid phase (SILP) catalysts for ethylene hydroformylation, Catal. Commun. 25 (2012) 136–141, https://doi.org/10.1016/j.catcom.2012.01.018.
[44] M. Jiang, L. Yan, Y. Ding, Q. Sun, J. Liu, H. Zhu, R. Lin, F. Xiao, Z. Jiang, J. Liu, Ultrastable 3V-PPh3 polymers supported single Rh sites for fixed-bed hydroformylation of olefins, J. Mol. Catal. A Chem. 404–405 (2015) 211–217, https://doi.org/10.1016/j.molcata.2015.05.008.
[45] S. Feng, M. Jiang, X. Song, P. Qiao, L. Yan, Y. Cai, B. Li, C. Li, L. Ning, S. Liu, W. Zhang, G. Wu, J. Yang, W. Dong, X. Yang, Z. Jiang, Y. Ding, Sulfur poisoning and self-recovery of single-site Rh 1 /porous organic polymer catalysts for olefin hydroformylation, Angew. Chem. Int. Ed. 62 (2023), https://doi.org/10.1002/anie.202304282.
[46] Y. Ding, L. Yan, X. Song, The Multifunctional Materials for Heterogenous Carboxylation: From Fundamental Understanding to Industrial Applications. Chem. Transform. C1 Compd., Wiley, 2022, pp. 289–324, https://doi.org/10.1002/9783527831883.ch7.
[47] F. Zaera, Key unanswered questions about the mechanism of olefin hydrogenation catalysis by transition-metal surfaces: a surface-science perspective, Phys. Chem. Chem. Phys. 15 (2013) 11988, https://doi.org/10.1039/c3cp50402f.
[48] J. Li, Q. Guan, H. Wu, W. Liu, Y. Lin, Z. Sun, X. Ye, X. Zheng, H. Pan, J. Zhu, S. Chen, W. Zhang, S. Wei, J. Lu, Highly active and stable metal single-atom catalysts achieved by strong electronic metal–support interactions, J. Am. Chem. Soc. 141 (2019) 14515–14519, https://doi.org/10.1021/jacs.9b06482.
[49] K. Maiti, S. Maiti, M.T. Curnan, H.J. Kim, J.W. Han, Engineering single atom catalysts to tune properties for electrochemical reduction and evolution reactions, Adv. Energy Mater. 11 (2021) 2101670, https://doi.org/10.1002/aenm.202101670.
[50] J. Yang, Y. Huang, H. Qi, C. Zeng, Q. Jiang, Y. Cui, Y. Su, X. Du, X. Pan, X. Liu, W. Li, B. Qiao, A. Wang, T. Zhang, Modulating the strong metal-support interaction of single-atom catalysts via vicinal structure decoration, Nat. Commun. 13 (2022) 4244, https://doi.org/10.1038/s41467-022-31966-1.
[51] M.J. Hülsey, S. Wang, B. Zhang, S. Ding, N. Yan, Approaching molecular definition on oxide-supported single-atom catalysts, Acc. Chem. Res. 56 (2023) 561–572, https://doi.org/10.1021/acs.accounts.2c00728.
[52] J. Amsler, B.B. Sarma, G. Agostini, G. Prieto, P.N. Plessow, F. Studt, Prospects of heterogeneous hydroformylation with supported single atom catalysts, J. Am. Chem. Soc. 142 (2020) 5087–5096, https://doi.org/10.1021/jacs.9b12171.
[53] I. Ro, M. Xu, G.W. Graham, X. Pan, P. Christopher, Synthesis of heteroatom Rh–ReOx atomically dispersed species on Al2O3 and their tunable catalytic

reactivity in ethylene hydroformylation, ACS Catal. 9 (2019) 10899–10912, https://doi.org/10.1021/acscatal.9b02111.

[54] S. Lee, A. Patra, P. Christopher, D.G. Vlachos, S. Caratzoulas, Theoretical study of ethylene hydroformylation on atomically dispersed Rh/Al 2 O 3 catalysts: reaction mechanism and influence of the ReO x promoter, ACS Catal. 11 (2021) 9506–9518, https://doi.org/10.1021/acscatal.1c00705.

[55] I. Ro, J. Qi, S. Lee, M. Xu, X. Yan, Z. Xie, G. Zakem, A. Morales, J.G. Chen, X. Pan, D.G. Vlachos, S. Caratzoulas, P. Christopher, Bifunctional hydroformylation on heterogeneous Rh-WOx pair site catalysts, Nature 609 (2022) 287–292, https://doi.org/10.1038/s41586-022-05075-4.

[56] M.G. Farpón, W. Henao, P.N. Plessow, E. Andrés, R. Arenal, C. Marini, G. Agostini, F. Studt, G. Prieto, Rhodium single-atom catalyst design through oxide support modulation for selective gas-phase ethylene hydroformylation, Angew. Chem. Int. Ed. 62 (2023), https://doi.org/10.1002/anie.202214048.

[57] L. Liu, U. Díaz, R. Arenal, G. Agostini, P. Concepción, A. Corma, Generation of subnanometric platinum with high stability during transformation of a 2D zeolite into 3D, Nat. Mater. 16 (2017) 132–138, https://doi.org/10.1038/nmat4757.

[58] T. Otto, S.I. Zones, E. Iglesia, Challenges and strategies in the encapsulation and stabilization of monodisperse Au clusters within zeolites, J. Catal. 339 (2016) 195–208, https://doi.org/10.1016/j.jcat.2016.04.015.

[59] J. Zhu, R. Osuga, R. Ishikawa, N. Shibata, Y. Ikuhara, J.N. Kondo, M. Ogura, J. Yu, T. Wakihara, Z. Liu, T. Okubo, Ultrafast encapsulation of metal nanoclusters into mfi zeolite in the course of its crystallization: catalytic application for propane dehydrogenation, Angew. Chem. Int. Ed. 59 (2020) 19669–19674, https://doi.org/10.1002/anie.202007044.

[60] L. Qi, S. Das, Y. Zhang, D. Nozik, B.C. Gates, A.T. Bell, Ethene hydroformylation catalyzed by rhodium dispersed with zinc or cobalt in silanol nests of dealuminated zeolite beta, J. Am. Chem. Soc. 145 (2023) 2911–2929, https://doi.org/10.1021/jacs.2c11075.

[61] M. Zhao, C. Li, D. Gómez, F. Gonell, V.M. Diaconescu, L. Simonelli, M.L. Haro, J. J. Calvino, D.M. Meira, P. Concepción, A. Corma, Low-temperature hydroformylation of ethylene by phosphorous stabilized Rh sites in a one-pot synthesized Rh-(O)-P-MFI zeolite, Nat. Commun. 14 (2023) 7174, https://doi.org/10.1038/s41467-023-42938-4.

[62] D.M. Hood, R.A. Johnson, A.E. Carpenter, J.M. Younker, D.J. Vinyard, G. G. Stanley, Highly active cationic cobalt(II) hydroformylation catalysts, Science 367 (80) (2020) 542–548, https://doi.org/10.1126/science.aaw7742.

[63] S. Tao, D. Yang, M. Wang, G. Sun, G. Xiong, W. Gao, Y. Zhang, Y. Pan, Single-atom catalysts for hydroformylation of olefins, IScience 26 (2023) 106183, https://doi.org/10.1016/j.isci.2023.106183.

[64] F. Hebrard, P. Kalck, Cobalt-catalyzed hydroformylation of alkenes: generation and recycling of the carbonyl species, and catalytic cycle, Chem. Rev. 109 (2009) 4272–4282, https://doi.org/10.1021/cr8002533.

[65] Z. Mao, Z. Xie, J.G. Chen, Comparison of heterogeneous hydroformylation of ethylene and propylene over RhCo3/MCM-41 catalysts, ACS Catal. 11 (2021) 14575–14585, https://doi.org/10.1021/acscatal.1c04359.

[66] K. Takeuchi, T. Hanaoka, T. Matsuzaki, M. Reinikainen, Y. Sugi, Selective vapor phase hydroformylation of ethylene over cluster-derived cobalt catalyst, Catal. Lett. 8 (1991) 253–261, https://doi.org/10.1007/BF00764124.

[67] N. Navidi, J.W. Thybaut, G.B. Marin, Experimental investigation of ethylene hydroformylation to propanal on Rh and Co based catalysts, Appl. Catal. A Gen. 469 (2014) 357–366, https://doi.org/10.1016/j.apcata.2013.10.019.

[68] D. Evans, J.A. Osborn, F.H. Jardine, G. Wilkinson, Homogeneous hydrogenation and hydroformylation using ruthenium complexes, Nature 208 (1965) 1203–1204, https://doi.org/10.1038/2081203b0.

[69] L. Huang, Y. Xu, Synergy of ruthenium and cobalt in SiO2-supported catalysts on ethylene hydroformylation, Appl. Catal. A Gen. 205 (2001) 183–193, https://doi.org/10.1016/S0926-860X(00)00573-1.

[70] L. Huang, Y. Xu, Studies on the interaction between ruthenium and cobalt in supported catalysts in favor of hydroformylation, Catal. Lett. 69 (2000) 145–151, https://doi.org/10.1023/A:1019050829687.

[71] H. Gong, X. Zhao, Y. Qin, W. Xu, X. Wei, Q. Peng, Y. Ma, S. Dai, P. An, Z. Hou, Hydroformylation of olefins catalyzed by single-atom Co(II) sites in zirconium phosphate, J. Catal. 408 (2022) 245–260, https://doi.org/10.1016/j.jcat.2022.03.011.

[72] F.J. Escobar-Bedia, M. Lopez-Haro, J.J. Calvino, V. Martin-Diaconescu, L. Simonelli, V. Perez-Dieste, M.J. Sabater, P. Concepción, A. Corma, Active and regioselective Ru single-site heterogeneous catalysts for alpha-olefin hydroformylation, ACS Catal. 12 (2022) 4182–4193, https://doi.org/10.1021/acscatal.1c05737.

[73] W. Gao, S. Liu, Z. Wang, J. Peng, Y. Zhang, X. Yuan, X. Zhang, Y. Li, Y. Pan, Outlook of cobalt-based catalysts for heterogeneous hydroformylation of olefins: from nanostructures to single atoms, Energy Fuels 38 (2024) 2526–2547, https://doi.org/10.1021/acs.energyfuels.3c03037.

[74] M. Ichiwaka, Catalytic hydroformylation of olefins over the rhodium, bimetallic RhCo, and cobalt carbonyl clusters supported with some metal oxides, J. Catal. 59 (1979) 67–78, https://doi.org/10.1016/S0021-9517(79)80046-9.

[75] C. Li, L. Yan, L. Lu, K. Xiong, W. Wang, M. Jiang, J. Liu, X. Song, Z. Zhan, Z. Jiang, Y. Ding, Single atom dispersed Rh-biphephos&PPh 3 @porous organic copolymers: highly efficient catalysts for continuous fixed-bed hydroformylation of propene, Green. Chem. 18 (2016) 2995–3005, https://doi.org/10.1039/C6GC00728G.

[76] A. Riisager, R. Fehrmann, M. Haumann, B.S.K. Gorle, P. Wasserscheid, Stability and kinetic studies of supported ionic liquid phase catalysts for hydroformylation of propene, Ind. Eng. Chem. Res. 44 (2005) 9853–9859, https://doi.org/10.1021/ie050629g.

[77] A. Riisager, R. Fehrmann, S. Flicker, R. van Hal, M. Haumann, P. Wasserscheid, Very stable and highly regioselective supported ionic-liquid-phase (SILP) catalysis: continuous-flow fixed-bed hydroformylation of propene, Angew. Chem. Int. Ed. 44 (2005) 815–819, https://doi.org/10.1002/anie.200461534.

[78] L. Alvarado Rupflin, J. Mormul, M. Lejkowski, S. Titlbach, R. Papp, R. Gläser, M. Dimitrakopoulou, X. Huang, A. Trunschke, M.G. Willinger, R. Schlögl, F. Rosowski, S.A. Schunk, Platinum group metal phosphides as heterogeneous catalysts for the gas-phase hydroformylation of small olefins, ACS Catal. 7 (2017) 3584–3590, https://doi.org/10.1021/acscatal.7b00499.

[79] Y. Zheng, Q. Wang, Q. Yang, S. Wang, M.J. Hülsey, S. Ding, S. Furukawa, M. Li, N. Yan, X. Ma, Boosting the hydroformylation activity of a Rh/CeO 2 single-atom catalyst by tuning surface deficiencies, ACS Catal. 13 (2023) 7243–7255, https://doi.org/10.1021/acscatal.3c00810.

[80] R. Lang, T. Li, D. Matsumura, S. Miao, Y. Ren, Y.-T. Cui, Y. Tan, B. Qiao, L. Li, A. Wang, X. Wang, T. Zhang, Hydroformylation of olefins by a rhodium single-atom catalyst with activity comparable to RhCl(PPh3)3, Angew. Chem. Int. Ed. 55 (2016) 16054–16058, https://doi.org/10.1002/anie.201607885.

[81] Z. Freixa, P.W.N.M. van Leeuwen, Bite angle effects in diphosphine metal catalysts: steric or electronic? Dalt. Trans. (2003) 1890–1901, https://doi.org/10.1039/B300322C.

[82] L. Yan, Y.J. Ding, H.J. Zhu, J.M. Xiong, T. Wang, Z.D. Pan, L.W. Lin, Ligand modified real heterogeneous catalysts for fixed-bed hydroformylation of propylene, J. Mol. Catal. A Chem. 234 (2005) 1–7, https://doi.org/10.1016/j.molcata.2005.01.047.

[83] T. Kim, F.E. Celik, D.G. Hanna, S. Shylesh, S. Werner, A.T. Bell, Gas-phase hydroformylation of propene over silica-supported PPh3-modified rhodium catalysts, Top. Catal. 54 (2011) 299–307, https://doi.org/10.1007/s11244-011-9664-3.

[84] S. Shylesh, D. Hanna, A. Mlinar, X.-Q. Kǒng, J.A. Reimer, A.T. Bell, In situ formation of wilkinson-type hydroformylation catalysts: insights into the structure, stability, and kinetics of triphenylphosphine- and xantphos-modified Rh/SiO 2, ACS Catal. 3 (2013) 348–357, https://doi.org/10.1021/cs3007445.

[85] L. Wang, W. Zhang, S. Wang, Z. Gao, Z. Luo, X. Wang, R. Zeng, A. Li, H. Li, M. Wang, X. Zheng, J. Zhu, W. Zhang, C. Ma, R. Si, J. Zeng, Atomic-level insights in optimizing reaction paths for hydroformylation reaction over Rh/CoO single-atom catalyst, Nat. Commun. 7 (2016) 14036, https://doi.org/10.1038/ncomms14036.

[86] M. Maestri, E. Iglesia, First-principles theoretical assessment of catalysis by confinement: NO–O 2 reactions within voids of molecular dimensions in siliceous crystalline frameworks, Phys. Chem. Chem. Phys. 20 (2018) 15725–15735, https://doi.org/10.1039/C8CP01615A.

[87] P. Ferri, C. Li, D. Schwalbe-Koda, M. Xie, M. Moliner, R. Gómez-Bombarelli, M. Boronat, A. Corma, Approaching enzymatic catalysis with zeolites or how to select one reaction mechanism competing with others, Nat. Commun. 14 (2023) 2878, https://doi.org/10.1038/s41467-023-38544-z.

[88] G. Sastre, A. Corma, The confinement effect in zeolites, J. Mol. Catal. A Chem. 305 (2009) 3–7, https://doi.org/10.1016/j.molcata.2008.10.042.

[89] B. Smit, T.L.M. Maesen, Towards a molecular understanding of shape selectivity, Nature 451 (2008) 671–678, https://doi.org/10.1038/nature06552.

[90] A. Corma, From microporous to mesoporous molecular sieve materials and their use in catalysis, Chem. Rev. 97 (1997) 2373–2420, https://doi.org/10.1021/cr960406n.

[91] J. Zhang, P. Sun, G. Gao, J. Wang, Z. Zhao, Y. Muhammad, F. Li, Enhancing regioselectivity via tuning the microenvironment in heterogeneous hydroformylation of olefins, J. Catal. 387 (2020) 196–206, https://doi.org/10.1016/j.jcat.2020.03.032.

[92] X. Zhang, T. Yan, H. Hou, J. Yin, H. Wan, X. Sun, Q. Zhang, F. Sun, Y. Wei, M. Dong, W. Fan, J. Wang, Y. Sun, X. Zhou, K. Wu, Y. Yang, Y. Li, Z. Cao, Regioselective hydroformylation of propene catalysed by rhodium-zeolite, Nature (2024), https://doi.org/10.1038/s41586-024-07342-y.

[93] B. Wei, J. Chen, X. Liu, K. Hua, L. Li, S. Zhang, H. Luo, H. Wang, Y. Sun, Achieving rhodium-like activity for olefin hydroformylation by electronic metal-support interaction of single atomic cobalt catalyst, Cell Rep. Phys. Sci. 3 (2022) 101016, https://doi.org/10.1016/j.xcrp.2022.101016.

[94] B. Wei, X. Liu, Q. Chang, S. Li, H. Luo, K. Hua, S. Zhang, J. Chen, Z. Shao, C. Huang, H. Wang, Y. Sun, Single-atom gold species within zeolite for efficient hydroformylation, Chem. Catal. 2 (2022) 2066–2076, https://doi.org/10.1016/j.checat.2022.06.008.

[95] G. Li, B. Wang, D.E. Resasco, Solvent effects on catalytic reactions and related phenomena at liquid-solid interfaces, Surf. Sci. Rep. 76 (2021) 100541, https://doi.org/10.1016/j.surfrep.2021.100541.

[96] N.S. Gould, S. Li, H.J. Cho, H. Landfield, S. Caratzoulas, D. Vlachos, P. Bai, B. Xu, Understanding solvent effects on adsorption and protonation in porous catalysts, Nat. Commun. 11 (2020) 1060, https://doi.org/10.1038/s41467-020-14860-6.

[97] Z. Yu, S. Zhang, L. Zhang, X. Liu, Z. Jia, L. Li, N. Ta, A. Wang, W. Liu, A. Wang, T. Zhang, Suppressing metal leaching and sintering in hydroformylation reaction by modulating the coordination of rh single atoms with reactants, J. Am. Chem. Soc. 146 (2024) 11955–11967, https://doi.org/10.1021/jacs.4c01315.

[98] D. Chandra, M.L. Garner, K.H. Lau, Vapor pressures of osmium, rhodium, and ruthenium carbonyls, J. Phase Equilibria. 20 (1999) 565–572, https://doi.org/10.1361/105497199770340554.

[99] F. Solymosi, M. Pasztor, An infrared study of the influence of carbon monoxide chemisorption on the topology of supported rhodium, J. Phys. Chem. 89 (1985) 4789–4793, https://doi.org/10.1021/j100268a026.

[100] F. Solymosi, J. Raskó, An infrared study of the influence of CO adsorption on the topology of supported ruthenium, J. Catal. 115 (1989) 107–119, https://doi.org/10.1016/0021-9517(89)90011-0.
[101] R. Dictor, S. Roberts, Morphological changes of rhodium on alumina as observed by using Fourier transform infrared spectroscopy, J. Phys. Chem. 93 (1989) 2526–2532, https://doi.org/10.1021/j100343a057.
[102] B.B. Sarma, P.N. Plessow, G. Agostini, P. Concepción, N. Pfänder, L. Kang, F. R. Wang, F. Studt, G. Prieto, Metal-specific reactivity in single-atom catalysts: CO oxidation on 4d and 5d transition metals atomically dispersed on MgO, J. Am. Chem. Soc. 142 (2020) 14890–14902, https://doi.org/10.1021/jacs.0c03627.
[103] P. Serna, B.C. Gates, Zeolite-supported rhodium complexes and clusters: switching catalytic selectivity by controlling structures of essentially molecular species, J. Am. Chem. Soc. 133 (2011) 4714–4717, https://doi.org/10.1021/ja111749s.
[104] A. Uzun, B.C. Gates, Dynamic structural changes in a molecular zeolite-supported iridium catalyst for ethene hydrogenation, J. Am. Chem. Soc. 131 (2009) 15887–15894, https://doi.org/10.1021/ja906553n.
[105] M.S. Peters, K.D. Timmerhaus, R.E. West, K. Timmerhaus, R. West, Plant Design and Economics for Chemical Engineers, McGraw-hill, New York, 1968.
[106] W.D. Seider, D.R. Lewin, J.D. Seader, S. Widagdo, R. Gani, K.M. Ng, Product and Process Design Principles: Synthesis, Analysis, and Evaluation, John Wiley & Sons, 2017.
[107] R. Turton, R.C. Bailie, W.B. Whiting, J.A. Shaeiwitz, Analysis, Synthesis and Design of Chemical Processes, Pearson Education, 2008.